Materials Advances

ROYAL SOCIETY OF CHEMISTRY

REVIEW

View Article Online
View Journal | View Issue



Cite this: *Mater. Adv.*, 2023, 4, 6478

# 2D layered double hydroxides and transition metal dichalcogenides for applications in the electrochemical production of renewable hydrogen

Daniele Alves,[a] P. Rupa Kasturi,[a] Gillian Collins,[a] Tara N Barwa,[a] Sukanya Ramaraj,[a] Raj Karthik [b] and Carmel B. Breslin *[ac]

The effects of Climate Change are now clearly evident across the world, with increasing storms, precipitation, rising sea levels and draughts, with an ever increasing need to develop energy storage and conversion approaches and devices to alleviate these issues. Hydrogen has emerged as a clean fuel with no environmental issues and it can be coupled with renewable energy sources such as wind, solar and wave energy. The excess energy from renewables can be employed to power electrolysis cells giving rise to green or renewable hydrogen. This approach is attracting considerable attention as it has the potential not only to provide a very clean energy source, but it also enables more efficient use of renewable energy resources. One of the limiting factors in achieving high volumes of pure hydrogen is the electrocatalytic materials used for the hydrogen evolution reaction (HER) and the oxygen evolution reaction (OER). In this review, we cover the progress made largely within the last six years in the development of two materials that satisfy the conditions of being cost-effective, earth-abundant, simple to form with little or no environmental concerns. The two materials are transition metal dichalcogenides (TMDs) and layered double hydroxides (LDHs), with the latter often described as clays. Following a short overview of the main synthetic methods used to form the TMDs and LDHs, and a short introduction to the HER and OER, the performance of different LDHs, TMDs and their composites in the electrochemical splitting of water, and as bifunctional electrodes is discussed. Finally, the ability of these materials to act as electrocatalysts in seawater electrolysis and to serve as electrocatalytic materials for the oxidation of alternative half-reactions to the sluggish OER is reviewed. Although more studies are required, it is clear that these earth-abundant materials are promising electrocatalysts for the generation of renewable hydrogen.

Received 8th September 2023,
Accepted 7th November 2023

DOI: 10.1039/d3ma00685a

rsc.li/materials-advances



## 1. Introduction

The effects of Climate Change are now clearly evident across the world, with dramatic changes emerging in the Earth's Climate.[1] It is expected that by the middle of the next century a temperature rise as high as 1.6 °C could be reached, leading to increased precipitation and rising sea levels, with major and negative economic, social and environmental impacts.[1,2] These effects are further compounded by the constant pursuit of modernisation with the development of new technologies that require extensive and ever-increasing global energy consumption. Accordingly, there has been a clear effort to reduce the use of fossil fuels and make a transition to investing in renewable energy resources, such as wind, wave, and solar energy.[3] However, these renewable resources are variable and intermittent in nature. They cannot be used to guarantee energy supply and therefore increasing the share of renewable energy to the energy grid is a challenging task and must be accompanied with efficient energy storage devices.

Some of the leading energy storage approaches include batteries,[4] supercapacitors[5] and hydrogen.[6] In particular, hydrogen has been recognised as a sustainable, clean, eco-friendly energy carrier with water as the only by-product when it is used in fuel cells and other applications. Currently, over 90% of the hydrogen comes from fossil fuel reforming and has no climate benefit as it generates $CO_2$. In contrast, electrolysis can be used to produce renewable (green) hydrogen. In this case, the excess or surplus energy from renewable energy resources,

[a] *Department of Chemistry, Maynooth University, Maynooth, Co, Kildare, Ireland. E-mail: Carmel.Breslin@mu.ie*
[b] *School of Chemical Engineering, Yeungnam University, Gyeongsan, Gyeongbuk 38541, Republic of Korea*
[c] *Kathleen Lonsdale Institute, Maynooth University, Maynooth, Co, Kildare, Ireland*

such as onshore and offshore wind and solar power, can be used to provide the energy needed in the electrolysis reaction. This makes electrolysis a promising, convenient, and environmentally acceptable method to generate renewable hydrogen. The splitting of water to give hydrogen and oxygen involves only three molecules, $H_2O$, $O_2$ and $H_2$, however it is a complex reaction, with various intermediates, adsorption and de-adsorption steps[7,8] and the electrocatalysts play a critically important role. Noble metal based electrocatalysts, centred on Pt, Ru and Ir, remain the most efficient for the splitting of water. However, these are very expensive with limited reserves.

In recent years there has been significant attention devoted to the development of new earth-abundant electrocatalysts for the hydrogen evolution reaction (HER) and the oxygen evolution reaction (OER). Various electrocatalysts have been considered, including different transition metal oxides,[9] MOF-derived oxides,[10] perovskites,[11] pyrochlore-type oxides,[12] transition metal carbides,[13] sulfides[10] and phosphides.[14] Among these emerging materials two-dimensional (2D) materials have attracted significant attention due to their unique electronic, optical, and catalytic properties, as well as their exceptional surface-to-volume ratios.[15,16] In particular, the transition metal dichalcogenides (TMDs),[17,18] and layered double hydroxides (LDHs)[19,20] have shown excellent potential as noble metal-free electrocatalysts for water splitting, since these materials are cost-effective, easily accessible, with facile fabrication methods. Additionally, they are abundant and rich in resources compared to the noble metal-based systems.[21]

The TMDs are a family of 2D materials comprising transition metal atoms (*e.g.*, Mo, W) sandwiched between chalcogen atoms (*e.g.*, S, Se). They have garnered significant interest in water splitting applications due to their intrinsic catalytic activity for both HER and OER, making them versatile catalysts in overall water-splitting systems.[22] Likewise, LDHs are a class of 2D materials with a layered structure consisting of divalent and trivalent metal cations, commonly Fe, Mn, Ni, Co and Cu with an interlayer charge compensating species, such as organic/inorganic anions and water molecules.[23] Their large surface area and interlayer spacing offer abundant active sites and easy ion diffusion, promoting efficient charge transport during the water-splitting process.[24] Although TMDs, and LDHs possess unique characteristics that can be utilised to improve the effectiveness of water-splitting reactions, there are certain drawbacks that require attention. These include low intrinsic activity, structural stability, limited active sites, and imbalanced catalytic performance.[25] As a solution, heterostructure materials have been proposed to overcome the aforementioned limitations, which not only preserve the essential features of the individual components, but engender novel properties arising from the synergistic effects of two or more materials as heterostructures.[26,27]

In this article, we review the recent developments in the application of TMDs and LDHs in the design of both HER and OER electrocatalysts. A comprehensive summary is provided on the research findings, arising mainly from the last six years, focusing on the predominant techniques employed to synthesise the TMDs, LDHs, and their composites, and their performance as HER, OER and as bifunctional electrocatalysts in the splitting of water. In addition, the performance of these 2D materials in seawater electrolysis and as electrocatalysts for alternative OER half-reactions, aiming to reduce the overall energy consumption, are described and discussed.

## 2. Summary of the main synthetic methods of 2D electrocatalytic materials

The properties and catalytic performance of 2D materials, such as TMDs and LDHs, are significantly influenced by the methods

**Daniele Alves**

*The authors are based in the Department of Chemistry at Maynooth University in Ireland and are dedicated to designing innovative functional materials for use in energy storage and conversion devices, electrochemical sensing and environmental applications. Professor Carmel Breslin, with research interests in electrochemistry and materials science, directs the group. Dr Rupa Kasturi Palanisamy, a postdoctoral researcher and Irish Research Council (IRC) fellow, is conducting research on 2D materials for energy storage and conversion devices. Dr Daniele Alves, a postdoctoral researcher funded by Science Foundation Ireland (SFI) works with LDHs and TMDs, for water-splitting and environmental applications. Dr Ramraj Sukanya, is a MSCA fellow, and is developing new metal dichalcogenides and oxides for electrochemical sensors and energy storage purposes. The doctoral candidates, Gillian Collins and Tara Barwa, with funding from IRC and SFI, concentrate on fabricating transition metal dichalcogenides and other 2D materials for water-splitting and electrochemical sensor applications. Lastly, Dr Raj Karthick, currently a visiting researcher with the group and research professor at Yeungnam University, in Korea, is working on advanced materials for energy-related applications. This group of researchers strives towards finding sustainable solutions for environmental and energy related applications and have published widely in these disciplines.*

employed during their synthesis.[28] The selection of an appropriate method is contingent upon various factors, including the specific material, desired properties, scalability, and intended applications in water-splitting devices.[29] Many methods have been applied to design and synthesise these materials individually, such as chemical vapor deposition (CVD),[30,31] mechanical exfoliation,[32] electrodeposition,[33] ion exchange[34] and co-precipitation,[35] while hydrothermal,[36] solvothermal,[37] and electrostatic self-assembly[38] are particularly useful in the synthesis of composites where two or more of these 2D materials are combined. This section elucidates the prevalent methods employed for the synthesis of composite 2D materials involving the TMDs and LDHs. The primary emphasis is on discussing the fabrication methods and their benefits for creating interfaces between these materials and integrating them with other nanostructures to enhance their charge separation and improve their catalytic performance.

### 2.1. Hydrothermal and solvothermal synthesis

The hydrothermal method involves subjecting the reaction system to elevated temperatures and pressures by employing water within a specially sealed container or autoclave.[39] The solvothermal process is analogous, however organic solvents, rather than water, or a combination of organic solvents with water, are used as the reaction medium. In comparison to alternative preparation techniques, these approaches are cost-effective concerning the use of raw materials, instrumentation, and energy consumption.[34] Additionally, the materials synthesised exhibit high purity and controlled morphology.[39] Consequently, these methods have garnered significant interest for synthesising TMDs, LDHs, and their respective composites.[40,41] As shown in Fig. 1, flower-like structures are often formed using the hydrothermal method.[42] However, other morphologies, such as $MoS_2$ nanorods,[43] nanoplates[44] and hollow nanoparticles,[45] and hexagonal and circular LDH platelets[46] can be formed by altering the temperature, time and nature of the precursors.

Hydrothermal processes are often combined with other methods due to several compelling reasons rooted in their synergistic benefits and enhanced material synthesis capabilities.[47,48] For example, Yang *et al.*[49] fabricated a CoFe–LDH/NiFe–LDH heterostructure supported on nickel foam (NF) using hydrothermal and electrodeposition methods. Firstly, the CoFe–LDH/NF was formed by a one-pot hydrothermal process, and then the NiFe–LDH was grown onto the surface of the CoFe–LDH/NF using electrodeposition. Notably, the hierarchical architecture featuring a ''nanosheet on nanosheet'' arrangement yielded an enhanced surface area, numerous active sites and an open porous network, thereby facilitating rapid mass transport and electrolyte penetration. Meanwhile, Chen *et al.* prepared NiFeCr–LDH/$MoS_2$ composites through co-precipitation and hydrothermal methods,[50] as illustrated in Fig. 2(a). Initially, NiFeCr–LDH was synthesized through co-precipitation using thiourea. Subsequently, the addition of

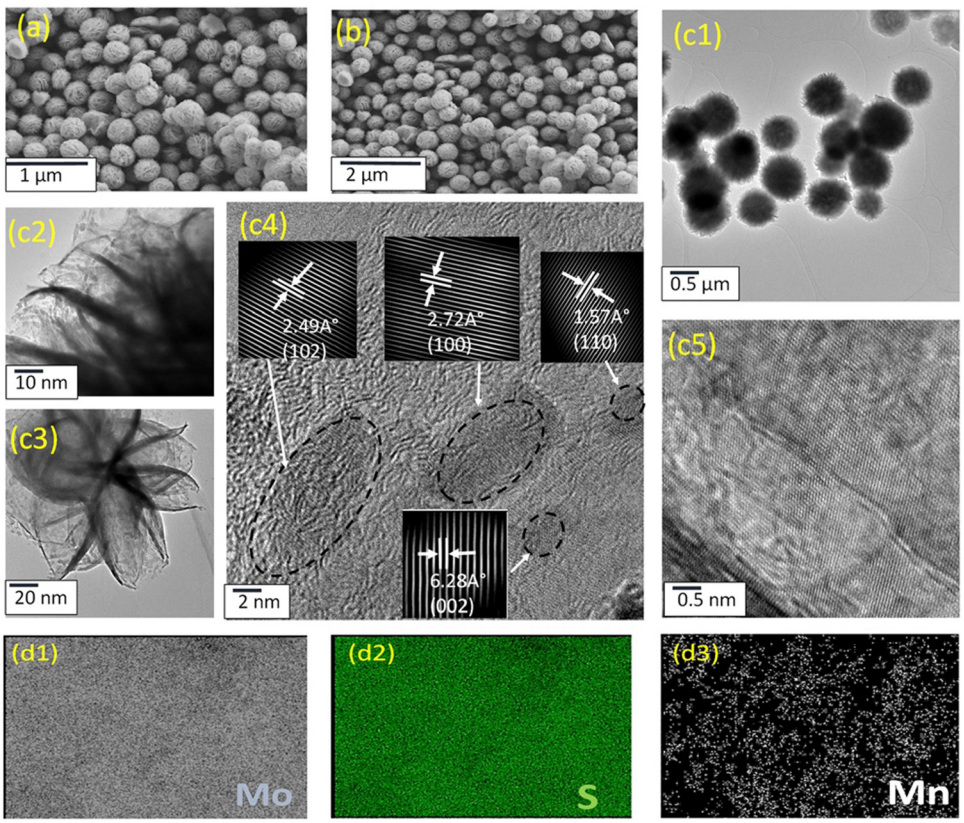


Fig. 1 Typical morphology obtained using hydrothermal/solvothermal synthesis, reprinted with permission from Elsevier, Shaikh *et al.*[42]

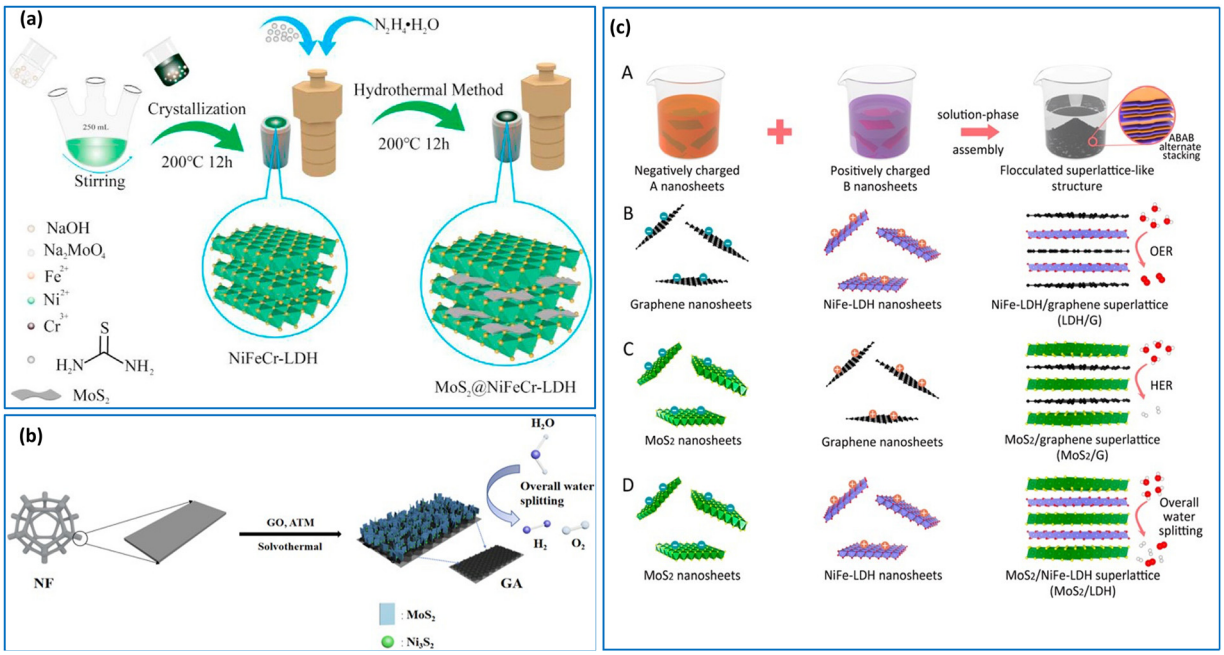


Fig. 2 (a) Schematic of the fabrication process of $MoS_2$/NiFeCr–LDH, reprinted with permission from Elsevier, Chen *et al.*,[50] (b) Illustration of the synthesis of $MoS_2/Ni_3S_2$/G/NF, reprinted with permission from Elsevier, Yu *et al.*,[26] (c) illustrations of (A) the synthesis by self-electrostatic-assembly of two kinds of unilamellar nanosheets with oppositely charged components, (B) LDH@G, (C) $MoS_2$@G and (D) $MoS_2$@LDH. Reprinted with permission from Xiong *et al.*,[59] Copyright 2019, American Chemical Society.

$MoO_4^{2-}$, followed by a reaction with sulfur and hydrazine hydrate, facilitated the generation of $MoS_2$ nanosheets within the interlayer spaces of NiFeCr–LDH. This interlayer confinement of NiFeCr–LDH played a pivotal role in the generation of the $MoS_2$ nanosheets, with a portion of the nanosheets adopting the 1T metallic phase, to give superior conductivity and enhanced electron transfer reactions. It is noteworthy that obtaining 1T $MoS_2$ nanosheets directly through the conventional hydrothermal method is challenging, underscoring the critical role of the confinement effect imparted by the LDH layers in this synthesis approach.

The solvothermal approach has been used to fabricate various heterostructures including graphene-templated $MoS_2$–$Ni_3S_2$ heterostructures, as shown in Fig. 2(b).[26] In this study, the graphene nanosheets were uniformly dispersed in DMF and heated, to facilitate a peeling process. This enabled the deposition of graphene, peeled into a few layers, onto the surface of nickel foam (NF) to enhance conductivity. The precursor compound, ammonium thiomolybdate ($(NH_4)_2MoS_4$), decomposes, yielding $MoS_3$, ammonia ($NH_3$), and hydrogen sulfide ($H_2S$). Subsequently, $MoS_3$ undergoes thermal decomposition to produce $MoS_2$ and elemental sulfur (S), which combines with the nickel foam substrate to give nickel sulfide ($Ni_3S_2$), culminating in the formation of a $MoS_2/Ni_3S_2$/G/NF heterostructure. This heterostructure engenders a synergistic effect, leading to a substantial augmentation in the population of active sites within the material. The interface established between the $MoS_2$ nanosheets and $Ni_3S_2$ nanoparticles facilitates the adsorption of both hydrogen and oxygen-containing intermediates, thereby enhancing the water hydrolysis reactions.

### 2.2. Electrostatic self-assembly

The electrostatic self-assembly stands out as the most basic approach for fabricating 2D materials and their composites.[51,52] This method predominantly relies on the electrostatic or van der Waals self-assembly principle, wherein cationic LDHs and anionic 2D materials, such as TMDs and graphene derivatives encompassing defective graphene (DG), and graphene oxide (GO) are readily electrostatically assembled.[53] The presence of defects in DG offers the potential for more efficient anchoring sites through strong π–π interactions, enabling direct coupling with transition metal atoms, thereby promoting rapid electron transfer kinetics, and imparting exceptional stability.[54] Furthermore, the most recent theoretical and experimental findings suggest that certain defect types in graphene and its derivatives can serve as active sites for OER and HER.[55–57] Recently, Jia *et al.*[58] anchored exfoliated NiFe–LDH nanosheets onto DG *via* electrostatic self-assembly. This entailed the exfoliation of NiFe–LDH to give single-layers of NiFe (LDH-NS), which are then self-assembled with the negatively charged DG. This approach was shown to enhance electron transfer and reduce diffusion distances through the manipulation of the graphene defects.

Likewise, TMDs have the capacity to intercalate with LDHs. Using a similar method, Xiong *et al.*[59] devised a solution-phase assembly process to synthesise NiFe–LDH/$MoS_2$, NiFe–LDH@graphene, and $MoS_2$@graphene heterostructures, as

shown in Fig. 2(c). This electrostatic assembly of LDHs and $MoS_2$ revealed the most potent interactions among adjacent layers within this cohort of hybrid materials. Indeed, the NiFe–LDH/$MoS_2$ exhibited advantageous adsorption energies for both the HER and OER intermediates and this was attributed to favourable electronic coupling effects at the heterointerfaces. These outcomes signify the prospects of interface modulation in superlattices as a facile and promising approach for the design of efficient electrocatalysts.

### 2.3. Exfoliation

Although CVD can be employed to give 2D TMDs, other methods such as hydrothermal and solvothermal methods produce 3D bulk structures for both the TMDs and LDHs, as shown in Fig. 1. The TMDs are readily exfoliated as the layers are held together by weak van der Waals forces and liquid–phase exfoliation (LPE) is normally used to give the 2D sheets. Organic solvents such as pyrrolidinone-based systems are very effective, but in more recent times, there has been more focus on using water-containing solvent systems and more environmentally acceptable systems such as ethanol and isopropanol.[60] However, the formation of 2D LDHs is more challenging as these layers are held by strong electrostatic interactions. A number of exfoliation approaches have been successfully employed to give 2D LDHs nanosheets and these include solvent systems such as deep eutectic solvents,[61] organic solvents such as formamide,[62,63] and formamide with $NH_4NO_3$ where the ammonium salt serves to increase the interlayer spacing.[62] Ethanol has also been used following pre-treatment of the as-synthesised LDH in a sodium acetate solution.[64] Indeed, it has been shown by Song and Hu that the higher OER activity of exfoliated LDHs can be traced to an increase in the number of active edge sites and improved electronic conductivity.[65] Nevertheless, the LDHs and TMDs are prone to restacking and agglomeration and are rarely used as single materials. By combining different families of 2D materials, as composites or heterostructures, these restacking processes can be inhibited, while the interface between both materials can facilitate and enhance the electron transfer process.

## 3. Hydrogen and oxygen evolution reactions and alternative half reactions

In the splitting of water, the HER serves as the reduction half reaction, and the OER provides the corresponding oxidation-half reaction. Both reactions require electrocatalytic materials that can not only promote the transfer of electrons, but can also facilitate the necessary adsorption and de-adsorption steps.[6] These adsorption and de-adsorption steps at the electrocatalysts can have a significant influence on both the HER and OER. If, too few intermediates bind to the electrocatalysts, due to weak interactions with the electrocatalyst, then the rate of the reaction will be slow. On the other hand, the reaction will also be slow if the adsorption is too strong, with the adsorbates failing to dissociate from the surface. The initial step in the HER is considered as the adsorption of hydrogen ions at the electrocatalytic sites and this is represented for acidic and basic media in eqn (1) and (2), respectively, where the symbol * indicates an adsorption site on Me (electrocatalyst site).[7,8] The main difference in these two equations is the source of the hydrogen atoms; provided as $H^+$ or $H_3O^+$ in the acidic medium and as $H_2O$ in an alkaline solution. In both cases, adsorbed hydrogen atoms are formed on the active surface sites of the electrocatalyst to give *Me–H. The gaseous $H_2(g)$ molecules can then be produced by combining two adjacently adsorbed hydrogen atoms, as illustrated in eqn (3). This is commonly described as the Tafel reaction. On the other hand, the adsorbed hydrogen atoms can couple with electrons and either a proton or water molecule, as shown for acidic and basic conditions in eqn (4) and (5), respectively, consistent with the Heyrovsky mechanism.

$$H^+(aq) + *Me + e^- \rightarrow *Me–H \text{ (Volmer)} \quad (1)$$

$$H_2O(l) + *Me + e^- \rightarrow *Me–H + OH^-(aq) \quad (2)$$

$$*Me–H + *Me–H \rightarrow *Me + *Me + H_2(g) \text{ (Tafel)} \quad (3)$$

$$*Me–H + H^+(aq) + e^- \rightarrow *Me + H_2(g) \text{ (Heyrovsky)} \quad (4)$$

$$*Me–H + H_2O(l) + e^- \rightarrow *Me + OH^-(aq) + H_2(g) \quad (5)$$

The corresponding OER is more kinetically sluggish and complex. In energy applications, the preferred OER is a four-electron, four-proton electron transfer process and can be represented as eqn (6) for alkaline solutions. The standard reduction potential of the OER is 1.23 V *vs.* SHE, however high overpotentials are needed to deliver the $O_2(g)$ molecules. This usually has a negative impact on the overall water splitting reaction with the overall efficiency being limited by the OER. The most widely accepted mechanism, which involves various intermediates, is the adsorbate evolution mechanism (AEM). The fundamental steps involved are illustrated in eqn (7)–(9) and involve bond breakage and formation reactions with oxygenated intermediates, such as *Me–OH, *Me–OOH and *Me–O. In addition to the relatively high overpotentials required for the OER, the electrocatalyst site (Me) is often susceptible to corrosion. In alkaline solutions and at high potentials, dissolution of the electrocatalyst can occur, through the formation of metal–oxygen intermediates, leading to the destabilisation of the electrocatalyst and the formation of water–soluble complexes.

$$*Me + OH^-(aq) \rightarrow *Me–OH + e^- \quad (6)$$

$$*Me–OH + OH^-(aq) \rightarrow *MeO + H_2O(l) + e^- \quad (7)$$

$$*Me–O + OH^-(aq) \rightarrow *Me–OOH + e^- \quad (8)$$

$$*Me–OOH + OH^-(aq) \rightarrow *Me + O_2(g) + H_2O(l) + e^- \quad (9)$$

The initial step in acidic solutions is the adsorption of the $H_2O$ molecule at the Me site. This is followed by water dissociation and the formation of Me–OH and finally M–O. In addition to acidic and alkaline media, there has been an increasing focus and interest in developing seawater electrolysis cells that can be

 

used on offshore wind farms.[66,67] Nevertheless, this remains a challenging process as the concentration of chloride in seawater is very high at approximately 0.5 M. Furthermore, the oxidation of chloride anions occurs at the anode to yield $Cl_2(g)$ under acidic conditions, while in alkaline solutions hypochlorite ions are formed. This oxidation reaction competes with the OER, and although the standard reduction potential for the oxidation of chloride to chlorine, at 1.36 V *vs.* SHE, is higher than the corresponding potential for OER, the oxidation of chloride has a relatively low overpotential. On the other hand, high overpotentials are needed to facilitate the OER and consequently, the evolution of chlorine can easily become the predominant reaction in acidic chloride-containing media. In addition, the corrosion of metal-based materials readily occurs in the presence of chloride anions.[68] Accordingly, the development of electrocatalysts for seawater electrolysis applications remains a challenging task, but is attracting increasing interest.[69,70]

As mentioned, the OER reaction is very sluggish and only occurs with high overpotentials, making the splitting of water and the production of hydrogen less efficient. Therefore, there has been much interest in finding alternative oxidation reactions that could replace the OER. One approach involves nucleophile oxidation reactions (NOR), with the oxidation of small organic molecules such as methanol and ethanol[71] as the anodic half-reactions. These oxidation reactions have lower onset potentials and lower energy consumption compared to the OER. Likewise, there is much interest in the hydrazine oxidation reaction (−0.33 V *vs.* RHE) where the only product is $N_2$. When this reaction is coupled with the HER, a much lower cell potential can be achieved and there is no risk of gaseous $O_2$ and $H_2$ combing.[72]

## 4. Assessment of the electrocatalysts for HER and OER

The electrocatalyst activity is normally measured using linear polarisation curves where the potential is extended into the hydrogen ion reduction or the oxygen evolution regions. The inclusion of a rotating disc can be beneficial in enabling the removal of hydrogen bubbles from the active surface sites, that otherwise would hinder the transport of the solution to the surface and increase the internal resistance. The experimental studies are generally performed in nitrogen or argon saturated electrolytes, and the potential is expressed using the reversible hydrogen electrode (RHE) scale, where $E_{(RHE)} = E_{(measured)} + E_{(ref\ used)} + 0.0591$ pH. Alternatively, solutions saturated with hydrogen gas for HER or oxygen gas for OER can be employed to avoid drifts in the equilibrium potential. However, the solutions usually become easily saturated with $H_2(g)$ or $O_2(g)$ and this is only an issue at low overpotentials, where the rate of $H_2(g)$ or $O_2(g)$ production is low. Parameters that are frequently employed to compare electrocatalysts are the overpotentials required to provide a current density of 10 mA $cm^{-2}$ (with the geometric surface area) and the Tafel slopes, Fig. 3. The Tafel slope can be obtained by fitting the experimental data to the Tafel region of the polarisation data and this gives information on how much overpotential is needed to increase the current density by an order of magnitude.[73] The Tafel equation is represented in eqn (10), where the slope (b) is equal to 2.303 $RT/\alpha F$ and the intercept (a) corresponds to $-(2.303\ RT/\alpha F)\log j_0$) for a reduction reaction, such as the HER. The other parameters have their usual meanings, with $R$ representing the gas constant, $F$ is the Faraday constant, $T$ is the thermodynamic temperature and $\alpha$ is the transfer coefficient. Tafel slopes in the vicinity of 120, 40 and 30 mV $dec^{-1}$ are typically assigned to Volmer, Heyrovsky and Tafel rate-determining steps, respectively.[74]

$$\eta = a + b\log j \tag{10}$$

Other parameters that are employed are the electrochemical active surface area (ECSA), Faraday Efficiency (FE), and turnover frequency (TOF). The ECSA value represents the specific surface area which gives a measure of the number of active sites. This involves measuring the double-layer capacitance of the electrocatalyst, which is then compared to the double-layer

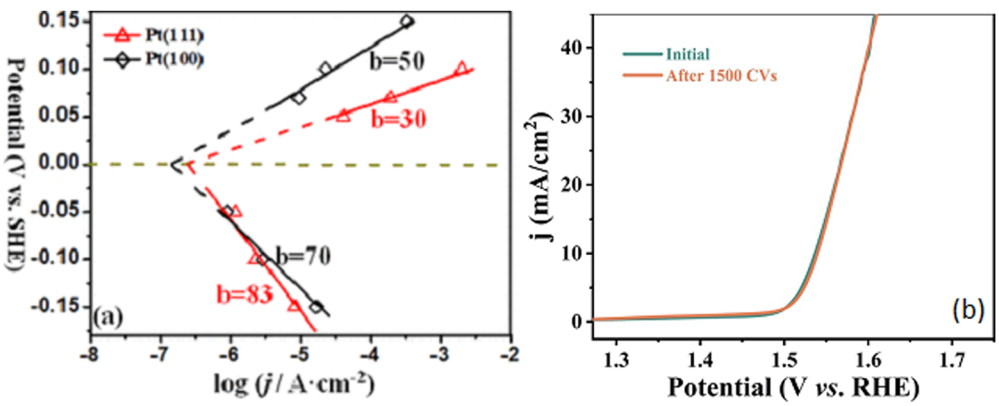


Fig. 3 (a) Typical Tafel plots showing oxidation and reduction half reactions for single crystal Pt, reprinted with permission from the American Chemical Society, Fang and Liu[73] (b) linear polarisation curves highlighting the stability of CoFe–LDH wrapped on Ni-doped carbon nanorods, reprinted with permission from Elsevier, Zhang and Hao.[75]

capacitance of a completely smooth surface, which is normally taken as 40 μC $cm^{-2}$, but can vary from 22 to 130 μC $cm^{-2}$ in alkaline solutions.[76] The FE represents the conversion efficiency and this is obtained by comparing the ratio of the experimentally determined amounts of $H_2$ or $O_2$ (usually by gas chromatography) to the theoretical yields. The theoretical data are obtained from chronoamperometric or chronopotentiometric measurements. The TOF represents the number of times the HER or OER occurs on a single site computed per unit time. It is typically computed using the geometric surface area, current density, number of electrons transferred, the Faraday constant, Avogadro's number, and the surface concentration of active sites which are involved in the reaction, as illustrated in eqn (11).

$$\mathrm{TOF} = \frac{j \times N_A}{F \times n \times \Gamma} \tag{11}$$

Nevertheless, all these parameters have limitations. The current is routinely normalised by the geometric surface area of the electrode, which can be very different to the real surface area, and in most cases underestimates the true surface area. Furthermore, determination of the actual number of active sites is difficult for supported electrocatalysts due to surface heterogeneity, facets and various crystallographic orientations. Also, many electrocatalysts undergo self-oxidation and possess significant capacitive behaviour, and this can have a significant effect on the overpotential values reported at 10 mA $cm^{-2}$. At higher currents, the overpotentials are less affected by secondary processes, but these are not always provided and IR drops have considerably more influence at higher current densities, making it difficult to compare different electrocatalysts. For Tafel analysis, a linear section of at least one decade of current and preferably two decades of current is needed to compute the Tafel slope,[73] while redox reactions associated with the electrocatalyst and mass-transport limitations can make this analysis more complex, making it sometimes difficult when comparing electrocatalysts in different studies.

# 5. 2D electrocatalysts for the production of hydrogen

As mentioned earlier, 2D layered materials, such as TMDs and LDHs, have emerged as promising electrocatalytic materials for the HER and the OER, as they have high surface areas, high density of active sites, good stability, are naturally abundant and are environmentally acceptable. For example, the LDHs are unique in the sense that their morphology, porosity, defective structure and intercalation can be easily adjusted during the preparation or synthetic steps. However, they suffer from low electrical conductivity and accordingly are normally combined with conducting materials, such as copper nanostructures,[77] carbon-based materials, including graphene,[78] rGO (reduced graphene oxide),[79] carbon nanotubes,[80] nanoporous carbon structures,[75] carbon nanofibers[81] and with semiconducting 2D materials, such as $MoS_2$,[82] $WS_2$[83] and various diselenides.[84]

In water splitting the electrolysis is typically carried out in strong acidic or alkaline conditions, as these conditions give rise to the lowest overpotentials. Nevertheless, this makes the conditions challenging in the design of electrocatalysts, as both the HER and OER electrocatalysts must be able to function in the same harsh electrolyte. Another more recent approach is to use a bifunctional electrocatalyst that can facilitate both the OER and HER making the electrolysis cells more economical and simpler in design.[85,86] Likewise, there is much interest in finding alternative oxidation-half reactions that could replace the sluggish OER half reaction,[87] while recent research is also focussed on using seawater as the medium.[88] These approaches are now described and discussed, highlighting the role of the 2D TMDs and LDHs in promoting the production of hydrogen.

## 5.1. Water splitting electrocatalysts

In general, the LDHs are very effective in promoting the OER, but are less studied for the HER as they have poor water dissociation kinetics (Volmer step).[89] They are always employed in alkaline solutions, such as 1.0 M KOH, as they dissolve in acidic media. On the other hand, the TMDs and their composites are very promising in promoting the HER in acidic[90] and basic solutions[91] and are also attracting increasing attention for their OER activities.[92–95] The LDHs, which contain the transition elements, Fe, Co, and Ni, are especially efficient in the OER half reaction and this is clearly evident in Table 1. Some of the lowest overpotentials are evident with the Fe and Ni systems. Indeed, the NiFe–LDH is considered as one of the best OER electrocatalysts.[96] Furthermore, they can be readily doped with additional cations and this has been recognised as an efficient avenue to improve the OER activity.[88]

Nevertheless, the precise elementary steps in the OER mechanism at LDHs still remains to be elucidated. Three mechanisms have been proposed and these include the adsorbate evolution mechanism (AEM), the intramolecular oxygen coupling (IMOC) and the lattice oxygen (LOC) mechanisms, as illustrated in Fig. 4. In a recent study, Wang *et al.*[97] employed modelling approaches to unravel the competing steps in the OER, including the role of applied potential, on M-doped Ni–LDHs, where M is Ni, Co and Fe. The authors concluded that the LOM mechanism occurs at the Ni–LDHs, but this mechanism is suppressed and the AEM mechanism is favoured when Fe is incorporated into the LDH. This can be advantageous as lattice oxygen is consumed through the LOM and this can give rise to dissolution reactions and long-term instability. It has also been shown that the LDHs can undergo transformations compared with their as-synthesised forms, during the OER. For example, Dionig *et al.*[98] demonstrated that Fe-based LDHs are converted from the as-prepared α-phase to the activated γ-phase with an 8% contraction of the lattice spacing. Likewise, phases such as γ-NiOOH, for Ni-based LDHs,[99] have been proposed to account for the impressive performance of these LDHs in the OER.

Table 1 Summary of the recent LDH and TMD-based electrocatalysts in the OER and HER half reactions

| Materials | Reaction electrolyte | $\eta$/mV | $B_c$/mV dec$^{-1}$ | Stability/h | Ref. |
|---|---|---|---|---|---|
| Zr–NiFe–LDH/NF | OER/KOH | 182 | 39 | 750 | 112 |
| Ni–C//CoFe–LDH/GCE | OER/KOH | 280 | 43 | 1500 cycles | 75 |
| NiFe–LDH/NF | OER/KOH | 225 | 42 | 60 | 113 |
| NiCo–LDH/FeOOH | OER/KOH | 255 | 82 | 73 | 114 |
| NiFe LDH/$MoS_2$ | OER/KOH | 190 | 31 | 45 | 82 |
| Ce–CoAl–LDH/$MoS_2$ | OER/KOH | 278 | 65 | — | 115 |
| $MoS_2$ quantum dots | OER/KOH | 370 | 39 | — | 116 |
| Fe–$MoS_2$/NF | OER/KOH | 230 | 78 | 140 | 117 |
| Cu–$MoS_2$/$NiS_2$ | HER/KOH | 105 | 59 | 1000 cycles | 118 |
| Cu–$MoS_2$/$NiS_2$ | HER/$H_2SO_4$ | 56 | 69 | 1000 cycles | 118 |
| Atomic C–$MoS_2$ | HER/$H_2SO_4$ | 87 | 45 | 72 | 119 |
| $CoS_2$/$MoS_2$ | HER/$H_2SO_4$ | 80 | 63 | 10 | 120 |
| $CoS_2$/$MoS_2$ | HER/KOH | 95 | 81 | 10 | 120 |
| $CoS_2$/$MoS_2$ | HER/neutral | 135 | 102 | 10 | 120 |
| $SnS_2$/$MoS_2$/$Ni_3S_2$/NF | HER/KOH | 232 | 107 | 100 | 91 |

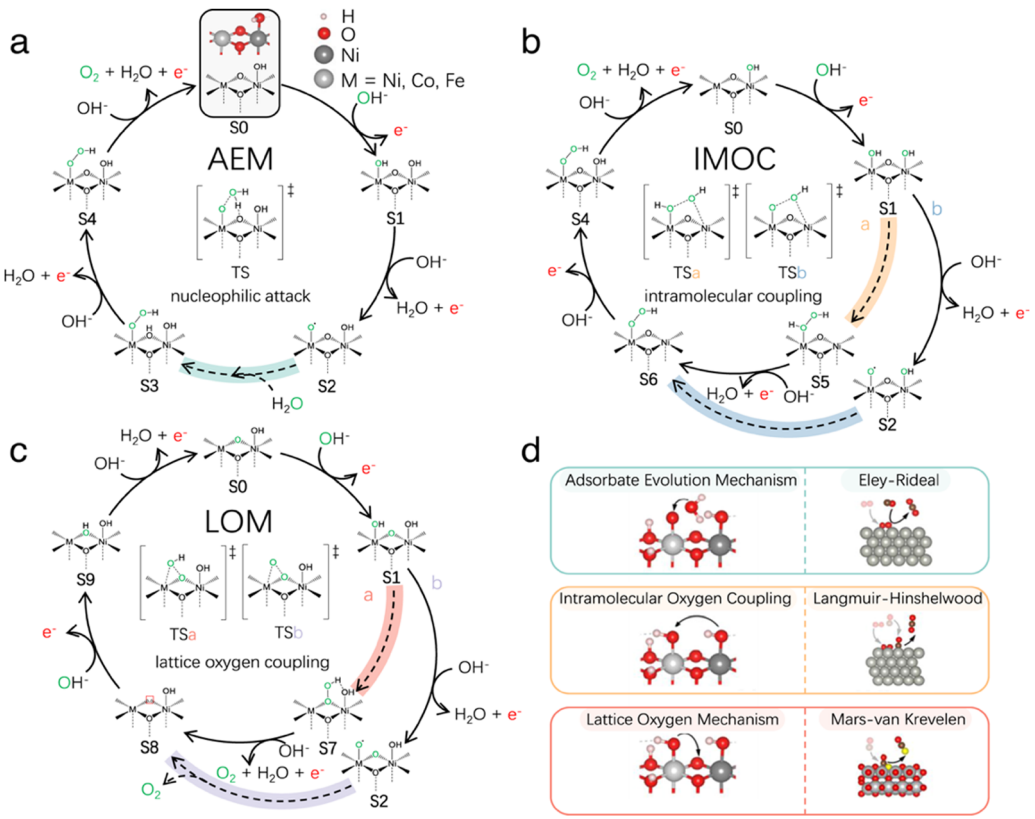


Fig. 4 Schematic of the reaction mechanisms for OER on Ni-based LDHs, (a) AEM, (b) IMOC, and (c) LOM mechanisms and (d) their association with heterogeneous catalysis mechanisms, taken from Wang *et al.*[97]

In addition, much research has been devoted to elucidating the HER mechanism at $MoS_2$ and to enhancing the HER activity, and some recent examples of $MoS_2$-based electrocatalysts in the HER and OER are shown in Table 1. It is generally accepted that the HER mechanism occurs through the Volmer–Heyrovsky pathway (eqn (1) and (4) at these materials.[100,101] However, one of the more significant challenges is optimising the charge-transfer processes. $MoS_2$ normally adopts the more thermodynamically stable 2H phase with the basal planes exhibiting very poor electrical conductivity. Three main approaches have been employed to enhance its electrocatalytic activity; (1) the introduction of higher densities of active edges through defect engineering, (2) conversion to the metastable 1T phase, through the intercalation of the 2H-$MoS_2$ lattice with, for example, lithium or organolithium compounds[102] and (3) formation of $MoS_2$ heterostructures or composites. It is clear that the 1T-$MoS_2$ phase has superior activity and this can be traced to the conducting basal planes of the 1T phase. Indeed,

Tang and Jiang[101] concluded from computational studies that the HER occurs at the basal plane of 1T-$MoS_2$. Nevertheless, it is difficult to maintain the $MoS_2$ in its non-thermodynamically stable 1T phase and various defect engineering strategies have emerged aiming to enhance the HER and OER activities. These include covalent functionalisation of the 1T phase with organic substituents with varying degrees of electron withdrawing and electron donating capacity to alter the charge density of the 1T-$MoS_2$ and minimise its transformation to the semiconducting 2H phase,[102] N-doping and $PO_4^{3-}$ intercalation to promote the conversion of 2H-$MoS_2$ to 1T-$MoS_2$,[103] desulfurisation to create high concentrations of S vacancies,[104] low-energy ion irradiation to form lattice defects[105] and doping with N,[106] F[107] and heteroatoms, such as transition metal atoms.[108–110] Similar approaches can be employed to enhance the charge-transfer processes for other family members, such as $MoSe_2$, $WS_2$, and $WSe_2$, and in turn promote the HER and OER. Although these are less well studied, there are reports that suggest that monolayer $MoSe_2$ with intrinsic defects and edges has real potential for the HER and OER reactions.[111]

Heterostructures, formed by combining two different materials with significant interfacial electronic interactions between the two interfaces, are emerging as new superior electrocatalytic materials, outperforming the single component counterparts. The performance of some of these heterostructures involving TMDs and LDHs in the OER and HER is summarised in Table 1. The heterostructures can provide electron transport channels, promoting efficient electron transfer throughout the heterostructures, while facilitating the adsorption/de-adsorption of essential reaction intermediates.

In addition to creating active sites, heterostructures, and enhancing the electronic conductivity of the LDHs and TMDs, the adhesion and accumulation of gas bubbles at the electrocatalyst surface requires developments. This can have a significant negative effect on the OER activity, preventing contact between the electrolyte and the electrocatalyst. Much research has been devoted to forming super-aerophobic type surfaces, that have the capacity to lower the adhesion between the surface and the forming bubbles. For example, Xie *et al.*[96] modified the surface of NiFe–LDH with the cationic surfactant, hexadecyl trimethyl ammonium bromide (CTAB), to increase the rate of bubble release. The corresponding OER current increased by a factor of 2.3. The surfactant formed a bilayer that not only reduced the adhesion of the bubbles, but the cationic groups facilitated and favoured the $OH^-$ adsorption step to give an increase in the OER activity. Many of the TMD-based electrocatalysts suffer from poor gaseous bubble detachment and removal. Recently, exciting surface engineering rationales to create super-aerophobicity and further improve the OER and HER in the TMD electrocatalysts have been developed. For example, it has been shown that the introduction of metal phosphides to give sulfide/phosphide heterostructures,[121] $CoSe_2/MoSe_2$ heterostructures[118] and the formation of wrinkled surface structures using shrink or pre-strained films[122] can be used to minimise bubble adhesion, as illustrated in Fig. 5.

### 5.2. Bifunctional electrocatalysts

The formation of bifunctional electrocatalysts that can serve as both the anodes and cathodes in the electrolysis cells is attractive, making the design of the electrolysis cell simpler and more cost-effective, with no need to match the electrocatalysts with specific pH values. Some of the recent results which highlight the performance of the TMDs, LDHs and their composites as bifunctional HER and OER electrocatalysts are summarised in Table 2 for alkaline cells. Some of the lowest cell potentials and lowest overpotentials are seen with TMD heterostructures, such as $MnCo_2S_4/MoS_2$[123] and transition metal-doped TMD heterostructures, such as Zr–$MoS_2/Ni_3S_2$.[124] Likewise, the LDHs perform well in this alkaline medium, with a FeCo–LDH/graphdiyne composite giving a cell potential at 10 mA $cm^{-2}$ of 1.43 V.[125] It is clear from Table 2 that carbon-based materials, such as graphdiyne can enhance the performance of LDHs. Carbon-based materials can not only enhance the electrical conductivity of the electrocatalysts, and protect it against corrosion reactions, but also promote the adsorption of $OH^-$ ions, eqn (6) and (7), which is essential to improve the OER activity. Other carbon-based materials that are combined with LDHs and TMDs to design bifunctional electrocatalysts include rGO.[126]

Most of the bifunctional $MoS_2$ and other TMD bifunctional electrocatalysts have been employed in alkaline media, such as KOH, Table 2. Nevertheless, hybrids including MWCNT/NiS/$MoS_2$,[127] Co–$MoS_2$/TiN,[128] Co–$MoS_2$/rGO,[129] and Co–$MoS_2$/CC (carbon cloth)[130] have been employed for the HER and OER half reactions in both acidic and alkaline media. Indeed, a cell potential of 1.55 V was obtained for the Co–$MoS_2$/CC in acidic solutions. Similarly, $MoS_2/Co_9S_8/Ni_3S_2/Ni$[131] has been employed as a bifunctional electrocatalyst over a wide pH range.

### 5.3. Seawater electrolysis

As mentioned earlier, seawater electrolysis is gaining considerable attention, and is now considered as one of the most sustainable approaches in the production of hydrogen. With the development of efficient seawater electrocatalysts, it becomes possible to generate high-purity hydrogen on offshore wind farms, making use of the largest water resource on earth. Nevertheless, the oxidation of chloride anions to generate chlorine-based compounds competes with the OER and this remains challenging. Other limiting factors in seawater electrolysis are associated with the high levels of chloride anions which promote corrosion and the presence of various ions that can give rise to insoluble precipitates, such as $Mg(OH)_2$ and $Ca(OH)_2$, at the electrocatalysts, which in turn block active sites. This makes the development of OER electrocatalysts that favour the OER over the oxidation of chloride anions, and that are stable over extended periods and not prone to corrosion in seawater, challenging. It has also been shown that $Br^-$ induced corrosion in seawater can be even more harmful to nickel-based electrocatalysts.[150] Typically, pitting corrosion is seen in the presence of $Cl^-$ ions with deep pits

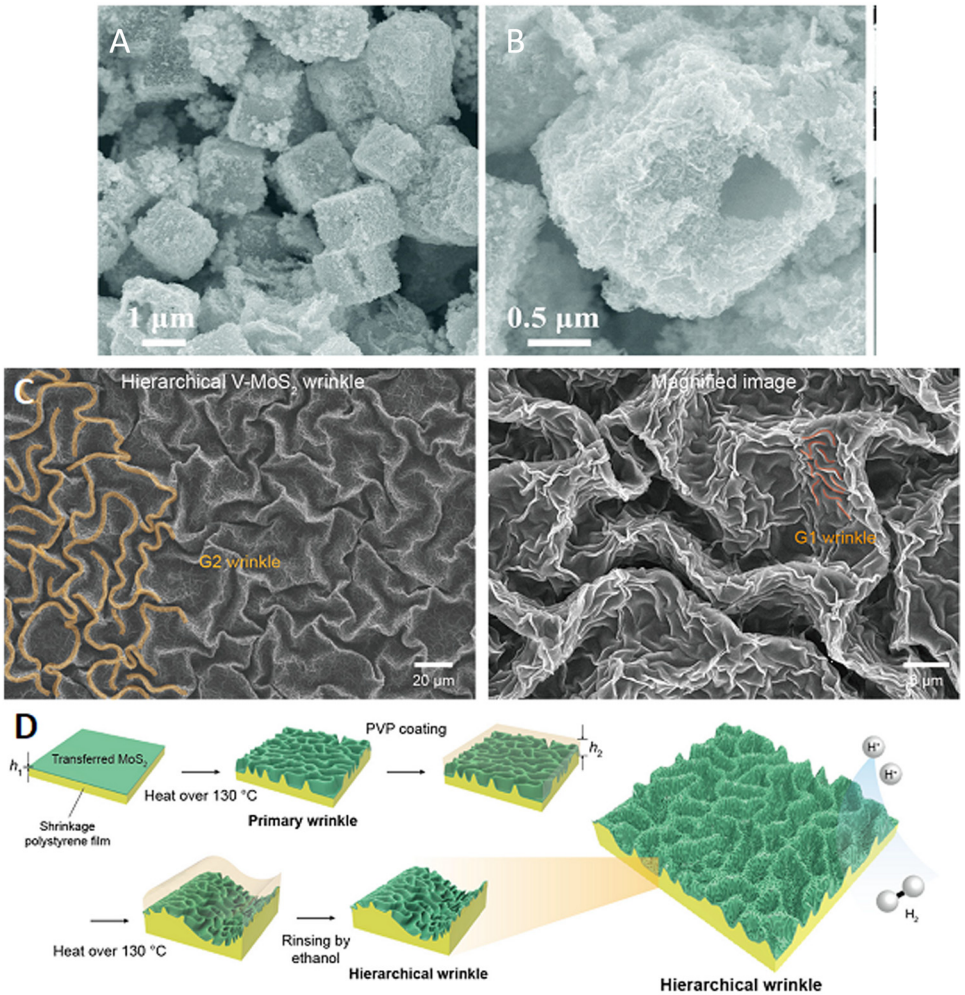


Fig. 5 Approaches employed to minimise the accumulation of gas bubbles at the electrocatalyst surface (A) and (B) $CoSe_2/MoSe_2$ heterostructures, reprinted with permission from the Royal Society of Chemistry, Chen *et al.*[118] and (C) wrinkled $VMoS_2$ and (D) schematic of the wrinkling procedure, reprinted with permission from the American Chemical Society, Jung *et al.*[122]

randomly decorated on the anode, while $Br^-$ etches more extensively to give shallow but wide pits that can consume the surface of the electrocatalyst with a more dramatic effect on stability.

Both the TMDs and LDHs have recently been considered in seawater electrolysis. Again, the main metal-based doping or elements involve Ni, Co and Fe.[151,152] For example, high-conducting CoNi nanowires were covered with $MoS_2$, and then atomically dispersed Pd and Ru were decorated over the $MoS_2$ to give a bifunctional electrocatalyst for both the HER and OER.[151] A cell potential of 1.54 V (at 10 mA $cm^{-2}$) in alkaline seawater was obtained with a 92% retention of the current over a 40 h period. It appears that the strong bonding interactions between the S and the Mo make the sulfide TMDs more corrosion resistant to chloride ion attack, and this can be important in terms of stability. Indeed, Song *et al.*[153] used a $MoS_2$ layer on the surface of $(FeNi)_9S_8$ to enhance the corrosion resistance of the composite in the presence of seawater. The $MoS_2/(FeNi)_9S_8$ hybrid was used as a bifunctional electrocatalyst. The authors concluded that in addition to good corrosion resistance, the heterogeneous interface facilitated the adsorption of H and OH intermediates, leading to improved electrocatalytic activity in the HER and OER.

In terms of the LDHs, they have also been employed in the electrolysis of alkaline seawater solutions. In this case, a recently reported partially selenised FeCo–LDH was successfully used in both the OER and HER.[154] The Se was used to hinder the diffusion of $Cl^-$ to the active sites, which served not only to reduce the corrosion processes and increase the lifetime of the electrocatalyst, but also to give high selectivity for the OER. Other materials, such as oxides sulfides and phosphides, carbides and nitrides have been combined with LDHs aiming to give both corrosion protection and the optimal adsorption free energy barriers of OH OOH intermediates to give improved OER activity. These include organophosphorus layers over NiCo–LDH to protect against corrosion.[155] Similarly, NiFe–LDHs have been combined with $CeO_2$,[156] $Cu_2S$,[157] $Ni_3Fe$,[158]

Table 2 Summary of the performance of some recent bifunctional electrocatalysts in KOH

| | $B_c$/mV dec$^{-1}$ | | $\eta$/mV | | | | |
|---|---|---|---|---|---|---|---|
| Materials | HER | OER | HER | OER | $E_{cell}/V$/mA cm$^{-2}$ | Stab./h | Ref. |
| $MoS_2$ nanolayers | 120 | 189 | 120 | 340 | — | — | 132 |
| $MnCo_2S_4/MoS_2$ | 26 | 53 | 70 | 160 | 1.41/10 | 20 | 123 |
| Zr–$MoS_2/Ni_3S_2$ | 61 | 79 | 98 | 275 | 1.49/10 | 50 | 124 |
| $MoS_2$–$Ni_3S_2$/NiFe–LDH | 62 | 108 | 12 | 220 | 1.50/10 | 50 | 133 |
| Co–$MoS_2/NiS_2$/CP | 81 | 99 | 109 | 323 | 1.67/10 | 24 | 134 |
| $MoS_2/NiS_2$ | 50 | 91 | 62 | 278 | 1.59/10 | 24 | 135 |
| Co–$MoS_2$ | 52 | 85 | 48 | 260 | — | — | 136 |
| $Co_3O_4/MoS_2$ | 98 | 45 | 205 | 230 | — | 10 | 137 |
| $MoS_2$–$NiS_2$/NGF | 70 | — | 68 | 370 | 1.64/10 | 24 | 138 |
| $Ni_3S_2$–$MoS_2$/FeOOH | 85 | 49 | 95 | 234 | 1.57/10 | 50 | 139 |
| $MoO_2$–$MoS_2/Co_9S_8$ | 80 | 70 | 160 | 310 | 1.62/10 | 20 | 140 |
| CoFe–LDH/NiFe–LDH | 89 | 46 | 160 | 240 | 1.59/10 | — | 141 |
| FeCo–LDH/graphdiyne | 99 | 44 | 43 | 216 | 1.43/10 | 60 | 125 |
| NiFe–LDH/CeOx | 101 | — | 154 | — | 1.51/10 | 10 | 142 |
| Ir–NiCo–LDH | 35 | 41 | 21 | 192 | 1.45/10 | 200 | 143 |
| CoMoV LDH | 182 | 106 | 150 | 270 | 1.61/10 | 20 | 144 |
| NiCoP/NiMn–LDH | 48 | 44 | 116 | 293 | 1.52/10 | 50 | 145 |
| CoMoP/NiFe–LDH | 93 | 55 | 99 | 225 | 1.68/50 | 27 | 146 |
| CuO/CoZn–LDH | 98 | 78 | 124 | 194 | 1.55/10 | 45 | 147 |
| Mo–NiCo LDH | 88 | 110 | 194 | 258 | 1.50/10 | 100 | 148 |
| NiFeZn LDH | 103 | 35 | 154 | 236 | 1.45/10 | 10 | 149 |

and $MnCo_2O_4$[159] to increase the corrosion protective properties of the composites.

Other approaches devised to impart corrosion resistance to the LDH electrocatalysts include the use of anionic corrosion inhibitors that are intercalated within the LDHs. Examples of suitable intercalated anionic inhibitors are $PO_4^{3-}$,[160] which are highly charged and can repel the anionic $Cl^-$ ions. In addition to the more commonly used Ni, Fe and Co LDHs, other elements including Co, Cr and V have been coupled to give layered triple hydroxides that can be used in alkaline seawater splitting.[88] In this case, the V gives higher concentrations of cationic active sites, while facilitating electronic transitions to favour the OER over the chloride evolution reaction.

### 5.4. Alternative oxidation half reactions to replace the OER

The sluggish kinetics and complex four-electron transfer process of the OER is a limiting half-reaction in the production of green hydrogen. An alternative approach is to couple the HER with other half-reactions that are more thermodynamically viable, with the aim of enhancing the production of pure hydrogen at a lower cost. Suitable half-reactions are the oxidation of urea,[161] various alcohols, such as ethanol,[162] aldehydes, amines, glycerol,[163] hydrazine[72] and products of biomass that have interesting and diverse applications.[164] The oxidation of urea is described in eqn (12), which has a considerably lower equilibrium potential of 0.37 V *vs.* RHE, compared with the OER. Despite its potential, it also suffers from slow kinetics as it involves the transfer of six electrons and the adsorption and de-adsorption of the NH and CO intermediates is also important in this reaction.

$$CO(NH_2)_2 + 6OH^- \rightarrow N_2 + CO_2 + 5H_2O + 6e^- \quad (12)$$

The influence of adding urea to the electrolysis cell is shown in Fig. 6, where it is clearly evident that a lower cell potential can be obtained when the oxidation of urea serves as the oxidation-half reaction. A number of LDH-modified

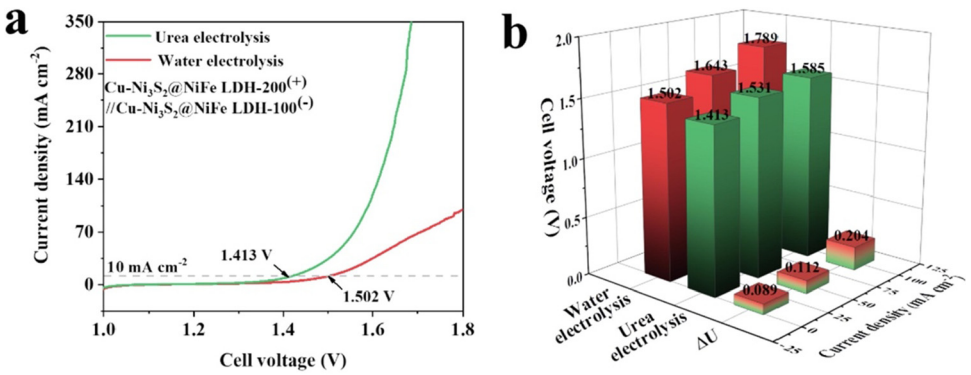


Fig. 6 (a) LSV curves and (b) cell potentials for the electrolysis of water and urea electrolysis with $\Delta U$ representing the difference in the cell potentials for Cu–$Ni_3S_2$@NiFe LDHs, reprinted with permission from Elsevier, Ding *et al.*[165]

electrocatalysts have been used to promote the oxidation of urea. As with the OER, the LDHs do not have a sufficiently high conductivity to promote the oxidation of urea and are normally combined with other components or modified or functionalised. For example, LDHs have been combined with sulfides, and noble metals, such as Cu–$Ni_3S_2$/NiFe LDH,[165] Rh/NiFe–LDH[166] and Au/NiCo−LDH.[167] Likewise, NiFe–LDHs have been oxidised using $H_2O_2$ to give a NiFeO–LDH catalyst that is superior to NiFe–LDHs.[168] In addition, their activity has been enhanced with a plasma functionalisation approach.[169] The nature of the intercalation anions seems to be relevant, with $NO_3^-$ intercalants in a NiCo–LDH giving the greatest activity and selectivity for the urea oxidation reaction.[170]

Another interesting approach is the use of bio-derived alcohols as the oxidation half-reaction in the formation of $H_2$.[171] This has the added advantage that valuable chemicals can be formed during the oxidation reaction. For instance, CoNi–LDH has been employed as the anode facilitating the electrochemical oxidation of urea, glycerol ethanol and benzyl alcohol, while the reduction of $H_2$ was achieved at a Pt-supported carbon cathode at a significantly reduced cell potential.[172] The oxidation products were identified as benzoate, acetate, and formate from the oxidation of benzyl alcohol, ethanol, and glycerol, respectively. Similarly, cobalt-based sulfides, including $CuCo_2S_4$[162] and $Co_3S_4$[173] have been employed as electrocatalysts for the ethanol oxidation reaction. Moreover, these Co-based sulfides exhibit very good HER performance, and can be employed as bifunctional electrocatalysts. Indeed, these ethanol-water electrolyser systems require relatively low cell potentials of 1.59 V[162] and 1.48 V[173] at a current density of 10 mA $cm^{-2}$.

## 6. Conclusions and future outlook

It is clear from this review that TMDs and LDHs have promising potential as electrocatalysts for the production of renewable hydrogen. Good progress has been made in their synthesis, with various hybrids, composites, and heterojunctions formed successfully. These materials have been shown to not only perform very well in alkaline conditions, but also studies have been reported in seawater media, highlighting the potential versatility of these 2D materials. More recently, the TMDs and LDHs are finding applications in promoting various oxidation half reactions as alternatives to the sluggish OER.

Nevertheless, the TMDs can be further improved by developing more efficient exfoliation methods and new avenues to halt the agglomeration of the exfoliated layers. Likewise, new methods are essential to increase the density of edge sites and to activate the basal plane of the 2H phases, which in turn would increase the electronic conductivity of this thermodynamically stable phase. The more conducting 1T-phase has relatively poor stability, making it difficult to maintain the conducting phase and prevent its transformation to the more thermodynamically favourable 2H phase. In addition, the long-term stability of the TMDs requires further study. There are different views on the nature of the active sites particularly when employed as OER electrocatalysts in alkaline conditions, with some authors arguing that the good OER activity is due to the formation of oxide phases, while others attribute the activity to the TMDs. The LDHs can only be used in alkaline media, as they dissolve and have poor stability in acidic or near acidic solutions. Again, the long-term stability of the LDHs is a potential issue, and like the TMDs, there are varying accounts of the active phases when cycled to high anodic potentials in OER applications. It remains difficult to exfoliate and maintain the LDHs as exfoliated layers due to the electrostatic interactions.

However, one of the greatest challenges facing the TMDs, LDHs and their composites/hybrids, and indeed other electrocatalysts, is their scale-up and performance in large scale industrial applications.[76] These materials satisfy the condition of cost-effectiveness. However, there are several aspects that require further development before their true potential to serve in cells, such as the membrane electrode assembly (MEA), or anion exchange membrane (AEM) electrolysers, can be evaluated:

(i) More emphasis is needed on the scale-up of their synthetic methods. Typically, the reported syntheses are carried out with mg to g quantities and scaling to kg or higher quantities can alter the properties and morphologies.

(ii) More considerations on the long term stability with continuous testing over weeks rather than the usual 20 h to gain greater insight into any transformations that may occur.

(iii) Assessment of the performance at current densities in the vicinity of 1 A $cm^{-2}$ as opposed to the much lower current densities of 10 mA $cm^{-2}$ that are normally used.

(iv) The adhesion and accumulation of gas bubbles at these materials require approaches aimed at minimising the adhesion of the bubbles. RDEs are used to remove the gaseous bubbles in small cells, but this is not possible in the MEAs and AEM electrolysers.

(v) The activity and performance of the electrocatalysts is normally assessed using small electrodes, such as glassy carbon electrode. While this is very useful in screening electrocatalysts and in obtaining fundamental information, the electrocatalysts may behave differently when coated onto porous substrates or membranes in the assembly of MEAs.

Furthermore, these materials are only beginning to be used in seawater. This is a challenging medium, but has huge potential in terms of off-shore wind farms where the hydrogen could be generated and stored. Relatively little is known about the chloride and indeed bromide-induced corrosion of both the TMDs and the LDHs and these studies are essential before these materials and their composites are used in this complex environment. Interestingly, they are beginning to be employed in the oxidation of various alcohols, urea, amines and biomass products that can serve as alternative half reactions to the sluggish OER that limits the overall efficiency of electrolysis cells.

While several challenges remain, both the TMDs, LDHs, and their composites and hybrids are interesting. They are cost

effective with little negative environmental impact. They can be conveniently combined with a variety of other conducting materials to enhance their performance and stability, and this is clearly an advantage of these layered materials.

## Author contributions

Daniele Alves: conceptualization, writing – original draft, writing – review & editing; P. Rupa Kasturi: conceptualization; visualization, writing – review & editing; Gillian Collins: conceptualization, writing – original draft, writing – review & editing; Tara N Barwa; writing – original draft, writing – review & editing; Sukanya Ramaraj: conceptualization, writing – review & editing; Raj Karthik: visualization, writing – review & editing; Carmel B. Breslin: conceptualization, writing – original draft, supervision, funding acquisition, writing – review & editing.

## Conflicts of interest

The authors declare that they have no conflict of interest in relation to the manuscript.

## Acknowledgements

This publication has emanated from research conducted with the financial support of Science Foundation Ireland under Grant number SFI/20/FFP-P/8793, the Irish Research Council under Grant numbers IRC/GOIPD/2022/694 and IRC/GOIPG/2022/1605 and from the European Union's Horizon 2020 research and innovation programme under the Marie Skłodowska-Curie grant agreement No 101106064.

## References

1 C. H. Trisos, C. Merow and A. L. Pigot, The projected timing of abrupt ecological disruption from climate change, *Nature*, 2020, **580**, 496, DOI: 10.1038/s41586-020-2189-9.

2 L. Cheng, J. Abraham, Z. Hausfather and K. E. Trenberth, How fast are the oceans warming, *Science*, 1979, **363**(2019), 128, DOI: 10.1126/science.aav7619.

3 P. A. Østergaard, N. Duic, Y. Noorollahi, H. Mikulcic and S. Kalogirou, Sustainable development using renewable energy technology, *Renewable Energy*, 2020, **146**, 2430, DOI: 10.1016/j.renene.2019.08.094.

4 Z. P. Cano, D. Banham, S. Ye, A. Hintennach, J. Lu, M. Fowler and Z. Chen, Batteries and fuel cells for emerging electric vehicle markets, *Nat. Energy*, 2018, **3**, 279, DOI: 10.1038/s41560-018-0108-1.

5 R. Sukanya, R. Karthik, M. Hasan, C. Breslin and J.-J. Shim, Insight into the synergistic effect of 2D/2D layered metal selenides wrapped nickel boride nanoparticles based ternary heterostructure for constructing asymmetric supercapacitors with excellent energy density, *Chem. Eng. J.*, 2023, **473**, 145487, DOI: 10.1016/j.cej.2023.145487.

6 R. Sukanya, D. C. da Silva Alves and C. B. Breslin, Review—Recent Developments in the Applications of 2D Transition Metal Dichalcogenides as Electrocatalysts in the Generation of Hydrogen for Renewable Energy Conversion, *J. Electrochem. Soc.*, 2022, **169**, 064504, DOI: 10.1149/1945-7111/ac7172.

7 J. Wei, M. Zhou, A. Long, Y. Xue, H. Liao, C. Wei and Z. J. Xu, Heterostructured electrocatalysts for hydrogen evolution reaction under alkaline conditions, *Nano-Micro Lett.*, 2018, **10**, 75, DOI: 10.1007/s40820-018-0229-x.

8 B. Mete, N. S. Peighambardoust, S. Aydin, E. Sadeghi and U. Aydemir, Metal-substituted zirconium diboride (Zr1-xTMxB2; TM = Ni, Co, and Fe) as low-cost and high-performance bifunctional electrocatalyst for water splitting, *Electrochim. Acta*, 2021, **389**, 138789, DOI: 10.1016/j.electacta.2021.138789.

9 J. S. Kim, B. Kim, H. Kim and K. Kang, Recent progress on multimetal oxide catalysts for the oxygen evolution reaction, *Adv. Energy Mater.*, 2018, **8**, 1702774, DOI: 10.1002/aenm.201702774.

10 H.-F. Wang, L. Chen, H. Pang, S. Kaskel and Q. Xu, MOF-derived electrocatalysts for oxygen reduction, oxygen evolution and hydrogen evolution reactions, *Chem. Soc. Rev.*, 2020, **49**, 1414, DOI: 10.1039/c9cs00906j.

11 Y. Chen, H. Li, J. Wang, Y. Du, S. Xi, Y. Sun, M. Sherburne, J. W. Ager, A. C. Fisher and Z. J. Xu, Exceptionally active iridium evolved from a pseudo-cubic perovskite for oxygen evolution in acid, *Nat. Commun.*, 2019, **10**, 572, DOI: 10.1038/s41467-019-08532-3.

12 P. Gayen, S. Saha and V. Ramani, Selective seawater splitting using pyrochlore electrocatalyst, *ACS Appl. Energy Mater.*, 2020, **3**, 3978, DOI: 10.1021/acsaem.0c00383.

13 Q. Gao, W. Zhang, Z. Shi, L. Yang and Y. Tang, Structural design and electronic modulation of transition-metal-carbide electrocatalysts toward efficient hydrogen evolution, *Adv. Mater.*, 2019, **31**, 1802880, DOI: 10.1002/adma.201802880.

14 L. Wu, L. Yu, F. Zhang, B. McElhenny, D. Luo, A. Karim, S. Chen and Z. Ren, Heterogeneous bimetallic phosphide Ni2PFe2P as an efficient bifunctional catalyst for water/seawater splitting, *Adv. Funct. Mater.*, 2021, **31**, 2006484, DOI: 10.1002/adfm.202006484.

15 H. Jin, C. Guo, X. Liu, J. Liu, A. Vasileff, Y. Jiao, Y. Zheng and S. Z. Qiao, Emerging two-dimensional nanomaterials for electrocatalysis, *Chem. Rev.*, 2018, **118**, 6337, DOI: 10.1021/acs.chemrev.7b00689.

16 Q. Quan and J. C. Ho, Recent advances in the construction of 2D heterostructures for electrocatalytic water splitting, *Adv. Energy Sustainability Res.*, 2022, **3**, 2200059, DOI: 10.1002/aesr.202200059.

17 M. Mohamed Abouelela, G. Kawamura and A. Matsuda, Metal chalcogenide-based photoelectrodes for photoelectrochemical water splitting, *J. Energy Chem.*, 2022, **73**, 189, DOI: 10.1016/j.jechem.2022.05.022.

18 S. Manzeli, D. Ovchinnikov, D. Pasquier, O. V. Yazyev and A. Kis, 2D transition metal dichalcogenides, *Nat. Rev. Mater.*, 2017, **2**, 17033, DOI: 10.1038/natrevmats.2017.33.

19 D. P. Sahoo, K. K. Das, S. Mansingh, S. Sultana and K. Parida, Recent progress in first row transition metal Layered double hydroxide (LDH) based electrocatalysts towards water splitting: A review with insights on synthesis, *Coord. Chem. Rev.*, 2022, **469**, 214666, DOI: 10.1016/j.ccr.2022.214666.

20 H. S. Jadhav, A. Roy, B. Z. Desalegan and J. G. Seo, An advanced and highly efficient Ce assisted NiFe–LDH electrocatalyst for overall water splitting, *Sustainable Energy Fuels*, 2019, **4**, 312, DOI: 10.1039/c9se00700h.

21 L. Sun, Q. Luo, Z. Dai and F. Ma, Material libraries for electrocatalytic overall water splitting, *Coord. Chem. Rev.*, 2021, **444**, 214049, DOI: 10.1016/j.ccr.2021.214049.

22 W. Choi, N. Choudhary, G. H. Han, J. Park, D. Akinwande and Y. H. Lee, Recent development of two-dimensional transition metal dichalcogenides and their applications, *Mater. Today*, 2017, **20**, 116, DOI: 10.1016/j.mattod.2016.10.002.

23 F. Liao, X. Zhao, G. Yang, Q. Cheng, L. Mao and L. Chen, Recent advances on two-dimensional NiFe–LDHs and their composites for electrochemical energy conversion and storage, *J. Alloys Compd.*, 2021, **872**, 159649, DOI: 10.1016/j.jallcom.2021.159649.

24 V. Kasneryk, M. Serdechnova, C. Blawert and M. L. Zheludkevich, LDH has been grown: What is next? Overview on methods of post-treatment of LDH conversion coatings, *Appl. Clay Sci.*, 2023, **232**, 106774, DOI: 10.1016/j.clay.2022.106774.

25 H. Zhong, Y. Feng and N. Alonso-Vante, Heterostructures based on transition metal chalcogenides and layered double hydroxides for enhanced water splitting, *Curr Opin Electrochem.*, 2022, **34**, 101016, DOI: 10.1016/j.coelec.2022.101016.

26 M. He, S. Hu, C. Feng, H. Liu and H. Mei, Interlaced rosette-like $MoS_2$/$Ni_3S_2$/NiFe–LDH grown on nickel foam: A bifunctional electrocatalyst for hydrogen production by urea-assisted electrolysis, *Int. J. Hydrogen Energy*, 2020, **45**, 23, DOI: 10.1016/j.ijhydene.2019.10.229.

27 H. Choi, S. Surendran, Y. Sim, M. Je, G. Janani, H. Choi, J. K. Kim and U. Sim, Enhanced electrocatalytic full water-splitting reaction by interfacial electric field in 2D/2D heterojunction, *Chem. Eng. J.*, 2022, **450**, 137789, DOI: 10.1016/j.cej.2022.137789.

28 H. Feng, J. Yu, L. Tang, J. Wang, H. Dong, T. Ni, J. Tang, W. Tang, X. Zhu and C. Liang, Improved hydrogen evolution activity of layered double hydroxide by optimizing the electronic structure, *Appl. Catal., B*, 2021, **297**, 120478, DOI: 10.1016/j.apcatb.2021.120478.

29 Q. Lv and R. Lv, Two-dimensional heterostructures based on graphene and transition metal dichalcogenides: Synthesis, transfer and applications, *Carbon*, 2019, **145**, 240, DOI: 10.1016/j.carbon.2019.01.008.

30 C. Lan, Z. Zhou, Z. Zhou, C. Li, L. Shu, L. Shen, D. Li, R. Dong, S. P. Yip and J. C. Ho, Wafer-scale synthesis of monolayer $WS_2$ for high-performance flexible photodetectors by enhanced chemical vapor deposition, *Nano Res.*, 2018, **11**, 3371, DOI: 10.1007/s12274-017-1941-4.

31 L. Cai and G. Yu, Recent advances in growth and modification of graphene-based energy materials: From chemical vapor deposition to reduction of graphene oxide, *Small Methods*, 2019, **3**, 1900071, DOI: 10.1002/smtd.201900071.

32 E. Gao, S. Z. Lin, Z. Qin, M. J. Buehler, X. Q. Feng and Z. Xu, Mechanical exfoliation of two-dimensional materials, *J. Mech. Phys. Solids*, 2018, **115**, 248, DOI: 10.1016/j.jmps.2018.03.014.

33 R. Li, Y. Li, P. Yang, D. Wang, H. Xu, B. Wang, F. Meng, J. Zhang and M. An, Electrodeposition: Synthesis of advanced transition metal-based catalyst for hydrogen production via electrolysis of water, *J. Energy Chem.*, 2021, **57**, 547, DOI: 10.1016/j.jechem.2020.08.040.

34 S. Alam, M. Asaduzzaman Chowdhury, A. Shahid, R. Alam and A. Rahim, Synthesis of emerging two-dimensional (2D) materials – Advances, challenges and prospects, *FlatChem*, 2021, **30**, 100305, DOI: 10.1016/j.flatc.2021.100305.

35 A. Urooj, M. Rani, A. A. Shah, S. Aslam, R. Siddiqui, A. Siddiqa, R. Neffati and A. D. Chandio, Morphological and optical investigation of 2D material-based ternary nanocomposite: $Bi_2O_3$/MgO/GO synthesized by a co-precipitation technique, *RSC Adv.*, 2022, **12**, 32986, DOI: 10.1039/d2ra04760h.

36 U. Alli, S. J. Hettiarachchi and S. Kellici, Chemical functionalisation of 2D materials by batch and continuous hydrothermal flow synthesis, *Chem. – Eur. J.*, 2020, **26**, 6447, DOI: 10.1002/chem.202000383.

37 J. Yu, Y. Zhang, J. Chen, L. Cui and W. Jing, Solvothermal-induced assembly of 2D-2D rGO-$TiO_2$ nanocomposite for the construction of nanochannel membrane, *J. Membr. Sci.*, 2020, **600**, 117870, DOI: 10.1016/j.memsci.2020.117870.

38 S. Zheng, S. Peng, Z. Wang, J. Huang, X. Luo, L. Han and X. Li, Schottky-structured 0D/2D composites via electrostatic self-assembly for efficient photocatalytic hydrogen evolution, *Ceram. Int.*, 2021, **47**, 28304, DOI: 10.1016/j.ceramint.2021.06.247.

39 X. Zhang, G. Ma and J. Wang, Hydrothermal synthesis of two-dimensional $MoS_2$ and its applications, *Tungsten*, 2019, **1**, 59, DOI: 10.1007/s42864-019-00014-9.

40 S. Ahmed, X. Ding, X. Chu, M. Li, D. Chu, T. Ma, T. Wu, A. Vinu and J. Yi, Shape and orientation controlled hydrothermal synthesis of silicide and metal dichalcogenide on a silicon substrate, *ACS Appl. Mater. Interfaces*, 2020, **12**, 18850, DOI: 10.1021/acsami.0c01222.

41 J. J. Huang, X. Q. Liu, F. F. Meng, L. Q. He, J. X. Wang, J. C. Wu, X. H. Lu, Y. X. Tong and P. P. Fang, A facile method to produce $MoSe_2$/MXene hybrid nanoflowers with enhanced electrocatalytic activity for hydrogen evolution, *J. Electroanal. Chem.*, 2020, **856**, 113727, DOI: 10.1016/j.jelechem.2019.113727.

42 N. Shaikh, I. Mukhopadhyay and A. Ray, Improved electrocatalytic hydrogen evolution characteristics in Mn-doped $MoS_2$ nanosheets grown under a non-equilibrium condition, *Int. J. Hydrogen Energy*, 2023, **48**, 15944, DOI: 10.1016/j.ijhydene.2023.01.098.

43 C. Zhang, H. B. Wu, Z. Guo and X. W. Lou, Facile synthesis of carbon-coated $MoS_2$ nanorods with enhanced lithium storage properties, *Electrochem. Commun.*, 2012, **20**, 7, DOI: 10.1016/j.elecom.2012.03.039.

44 H. Hwang, H. Kim and J. Cho, $MoS_2$ nanoplates consisting of disordered graphene-like layers for high rate lithium battery anode materials, *Nano Lett.*, 2011, **11**, 4826, DOI: 10.1021/nl202675f.

45 M. Wang, G. Li, H. Xu, Y. Qian and J. Yang, Enhanced lithium storage performances of hierarchical hollow $MoS_2$ nanoparticles assembled from nanosheets, *ACS Appl. Mater. Interfaces*, 2013, **5**, 1003, DOI: 10.1021/am3026954.

46 Y. Zhang, W. Xie, J. Ma, L. Chen, C. Chen, X. Zhang and M. Shao, Active facet determination of layered double hydroxide for oxygen evolution reaction, *J. Energy Chem.*, 2021, **60**, 127, DOI: 10.1016/j.jechem.2020.12.038.

47 Y. Zhang, S. C. Xue, X. H. Yan, H. L. Gao, X. Jing, K. Z. Gao, Y. Cao, H. W. Luo and J. Yan, Synthesis of CoAl–LDH@$Ni(OH)_2$ high-performance supercapacitor electrode composites by hydrothermal-assisted electrodeposition, *Ionics*, 2022, **28**, 5211, DOI: 10.1007/s11581-022-04743-9.

48 T. V. Thu and V. D. Thao, Influence of temperature on structure, morphology, and magnetic property of graphene–$MnFe_2O_4$ nanocomposites synthesized by a combined hydrothermal/co-precipitation method, *Appl. Phys. A: Mater. Sci. Process.*, 2018, **124**, 675, DOI: 10.1007/s00339-018-2092-5.

49 R. Yang, Y. Zhou, Y. Xing, D. Li, D. Jiang, M. Chen, W. Shi and S. Yuan, Synergistic coupling of CoFe–LDH arrays with NiFe–LDH nanosheet for highly efficient overall water splitting in alkaline media, *Appl. Catal., B*, 2019, **253**, 131–139, DOI: 10.1016/j.apcatb.2019.04.054.

50 S. Chen, C. Yu, Z. Cao, X. Huang, S. Wang and H. Zhong, Trimetallic NiFeCr–LDH/$MoS_2$ composites as novel electrocatalyst for OER, *Int. J. Hydrogen Energy*, 2021, **46**, 7037, DOI: 10.1016/j.ijhydene.2020.11.249.

51 J. E. Kim, J. H. Oh, M. Kotal, N. Koratkar and I. K. Oh, Self-assembly and morphological control of three-dimensional macroporous architectures built of two-dimensional materials, *Nano Today*, 2017, **14**, 100, DOI: 10.1016/j.nantod.2017.04.008.

52 X. Zhang, Y. Dong, F. Pan, Z. Xiang, X. Zhu and W. Lu, Electrostatic self-assembly construction of 2D $MoS_2$ wrapped hollow $Fe_3O_4$ nanoflowers@1D carbon tube hybrids for self-cleaning high-performance microwave absorbers, *Carbon*, 2021, **177**, 332, DOI: 10.1016/j.carbon.2021.02.092.

53 S. Nayak and K. Parida, Recent progress in LDH@Graphene and analogous heterostructures for highly active and stable photocatalytic and photoelectrochemical water splitting, *Chem. – Asian J.*, 2021, **16**, 2211, DOI: 10.1002/asia.202100506.

54 A. Gupta, T. Sakthivel and S. Seal, Recent development in 2D materials beyond graphene, *Prog. Mater. Sci.*, 2015, **73**, 44, DOI: 10.1016/j.pmatsci.2015.02.002.

55 J. Albero, D. Mateo and H. García, Graphene-based materials as efficient photocatalysts for water splitting, *Molecules*, 2019, **24**, 906, DOI: 10.3390/molecules24050906.

56 R. Wan, C. Wang, R. Chen, M. Liu and F. Yang, Enhanced catalytic activities of Fe anchored on graphene substrates for water splitting and hydrogen evolution, *Int. J. Hydrogen Energy*, 2022, **47**, 32039, DOI: 10.1016/j.ijhydene.2022.07.096.

57 X. Guo, S. Liu and S. Huang, Single Ru atom supported on defective graphene for water splitting: DFT and microkinetic investigation, *Int. J. Hydrogen Energy*, 2018, **43**, 4880, DOI: 10.1016/j.ijhydene.2018.01.122.

58 Y. Jia, L. Zhang, G. Gao, H. Chen, B. Wang, J. Zhou, M. T. Soo, M. Hong, X. Yan, G. Qian, J. Zou, A. Du and X. Yao, A Heterostructure coupling of exfoliated Ni–Fe hydroxide nanosheet and defective graphene as a bifunctional electrocatalyst for overall water splitting, *Adv. Mater.*, 2017, **29**, 1700017, DOI: 10.1002/adma.201700017.

59 P. Xiong, X. Zhang, H. Wan, S. Wang, Y. Zhao, J. Zhang, D. Zhou, W. Gao, R. Ma, T. Sasaki and G. Wang, Interface modulation of two-dimensional superlattices for efficient overall water splitting, *Nano Lett.*, 2019, **19**, 4518, DOI: 10.1021/acs.nanolett.9b01329.

60 Y. Luo, T. N. Barwa, K. Herdman, E. Dempsey and C. B. Breslin, Electroanalysis of metronidazole using exfoliated $MoS_2$ sheets and electrodeposited amorphous MoSx, *Electrochim. Acta*, 2023, **462**, 142778, DOI: 10.1016/j.electacta.2023.142778.

61 A. L. Siegel, L. Adhikari, S. Salik and G. A. Baker, Progress and prospects for deep eutectic solvents in colloidal nanoparticle synthesis, *Curr. Opin. Green Sustainable Chem.*, 2023, **41**, 100770, DOI: 10.1016/j.cogsc.2023.100770.

62 X. Bai, A. Shi, F. Zhang, Z. Jiang, D. Liao and H. Zhang, Preparation of Mg-Al layered double hydroxides ultrathin nanosheets and its application in adsorption of methyl orange, *Nano*, 2023, **18**, 2350020, DOI: 10.1142/S1793292023500200.

63 H. Zhao, L. Hu, L. Wang, J. Zhu, H. Cui and J. He, The structural feature of Ni–Al–LDH nanosheets and their adsorption performance for ethyl mercaptan from methane gas, *New J. Chem.*, 2022, **46**, 20235, DOI: 10.1039/d2nj03997d.

64 M. Piccinni, S. Bellani, G. Bianca and F. Bonaccorso, Nickel-iron layered double hydroxide dispersions in ethanol stabilized by acetate anions, *Inorg. Chem.*, 2022, **61**, 4598, DOI: 10.1021/acs.inorgchem.1c03485.

65 F. Song and X. Hu, Exfoliation of layered double hydroxides for enhanced oxygen evolution catalysis, *Nat. Commun.*, 2014, **5**, 4477, DOI: 10.1038/ncomms5477.

66 Y. Kuang, M. J. Kenney, Y. Meng, W.-H. Hung, Y. Liu, J. E. Huang, R. Prasanna, P. Li, Y. Li, L. Wang, M.-C. Lin, M. D. McGehee, X. Sun and H. Dai, Solar-driven, highly sustained splitting of seawater into hydrogen and oxygen fuels, *Proc. Natl. Acad. Sci. U. S. A.*, 2019, **116**, 6624, DOI: 10.1073/pnas.1900556116.

67 L. Wu, L. Yu, F. Zhang, B. McElhenny, D. Luo, A. Karim, S. Chen and Z. Ren, Heterogeneous bimetallic phosphide

Ni2P-Fe2P as an efficient bifunctional catalyst for water/seawater splitting, *Adv. Funct. Mater.*, 2021, **31**, 2006484, DOI: 10.1002/adfm.202006484.

68 F. Mansfeld, C. B. Breslin, A. Pardo and F. J. Pérez, Surface modification of stainless steels: Green technology for corrosion protection, *Surf. Coat. Technol.*, 1997, **90**, 224, DOI: 10.1016/S0257-8972(96)03142-8.

69 S. Feng, P. Rao, Y. Yu, J. Li, P. Deng, Z. Kang, S. Wang, Z. Miao, Y. Shen, X. Tian, X. Tian and Z. Wu, Self-assembled heterojunction $CoSe_2$@CoO catalysts for efficient seawater electrolysis, *Electrochim. Acta*, 2023, **463**, 142870, DOI: 10.1016/j.electacta.2023.142870.

70 Y. Gong, H. Zhao, Y. Sun, D. Xu, D. Ye, Y. Tang, T. He and J. Zhang, Partially selenized FeCo layered double hydroxide as bifunctional electrocatalyst for efficient and stable alkaline (sea)water splitting, *J. Colloid Interface Sci.*, 2023, **650**, 636, DOI: 10.1016/j.jcis.2023.07.013.

71 J. Shi, H. He, Y. Guo, F. Ji, J. Li, Y. Zhang, C. Deng, L. Fan and W. Cai, Enabling high-efficiency ethanol oxidation on NiFe–LDH via deprotonation promotion and absorption inhibition, *J. Energy Chem.*, 2023, **85**, 76, DOI: 10.1016/j.jechem.2023.06.011.

72 S. Zhang, C. Zhang, X. Zheng, G. Su, H. Wang and M. Huang, Integrating electrophilic and nucleophilic dual sites on heterogeneous bimetallic phosphide via enhancing interfacial electronic field to boost hydrazine oxidation and hydrogen evolution, *Appl. Catal., B*, 2023, **324**, 122207, DOI: 10.1016/j.apcatb.2022.122207.

73 Y.-H. Fang and Z.-P. Liu, Tafel kinetics of electrocatalytic reactions: From experiment to first-principles, *ACS Catal.*, 2014, **4**, 4364, DOI: 10.1021/cs501312v.

74 T. Shinagawa, A. T. Garcia-Esparza and K. Takanabe, Insight on Tafel slopes from a microkinetic analysis of aqueous electrocatalysis for energy conversion, *Sci. Rep.*, 2015, **5**, 13801, DOI: 10.1038/srep13801.

75 J. Zhang, L. Hao, Z. Chen, Y. Gao, H. Wang and Y. Zhang, Facile synthesis of Co–Fe layered double hydroxide nanosheets wrapped on Ni-doped nanoporous carbon nanorods for oxygen evolution reaction, *J. Colloid Interface Sci.*, 2023, **650**, 816, DOI: 10.1016/j.jcis.2023.06.199.

76 C. C. L. McCrory, S. Jung, J. C. Peters and T. F. Jaramillo, Benchmarking heterogeneous electrocatalysts for the oxygen evolution reaction, *J. Am. Chem. Soc.*, 2013, **135**, 16977, DOI: 10.1021/ja407115p.

77 L. Yu, H. Zhou, J. Sun, F. Qin, F. Yu, J. Bao, Y. Yu, S. Chen and Z. Ren, Cu nanowires shelled with NiFe layered double hydroxide nanosheets as bifunctional electrocatalysts for overall water splitting, *Energy Environ. Sci.*, 2017, **10**, 1820, DOI: 10.1039/c7ee01571b.

78 X. Long, J. Li, S. Xiao, K. Yan, Z. Wang, H. Chen and S. Yang, A strongly coupled graphene and FeNi double hydroxide hybrid as an excellent electrocatalyst for the oxygen evolution reaction, *Angew. Chem., Int. Ed.*, 2014, **53**, 7584, DOI: 10.1002/anie.201402822.

79 P. Zhang, L. Chen, L. Ge, P. Song, R. Xie, B. Wang, Y. Fu, S. Jia, T. Liao and Y. Xiong, A 3D rGO-supported NiFe2O4 heterostructure from sacrificial polymer-assisted exfoliation of NiFe–LDH for efficient oxygen evolution reaction, *Carbon*, 2022, **200**, 422, DOI: 10.1016/j.carbon.2022.08.085.

80 X. Yan, Z. Wang, J. Bao, Y. Song, X. She, J. Yuan, Y. Hua, G. Lv, H. Li and H. Xu, CoMo layered double hydroxide equipped with carbon nanotubes for electrocatalytic oxygen evolution reaction, *Nanotechnology*, 2023, **34**, 065401, DOI: 10.1088/1361-6528/ac9abd.

81 J. Xu, M. Wang, F. Yang, X. Ju and X. Jia, Self-supported porous Ni-Fe-W hydroxide nanosheets on carbon fiber: A highly efficient electrode for oxygen evolution reaction, *Inorg. Chem.*, 2019, **58**, 13037, DOI: 10.1021/acs.inorgchem.9b01953.

82 S. Chakraborty, S. Marappa, S. Agarwal, D. Bagchi, A. Rao, C. P. Vinod, S. C. Peter, A. Singh and M. Eswaramoorthy, Improvement in oxygen evolution performance of NiFe layered double hydroxide grown in the presence of 1T-rich $MoS_2$, *ACS Appl. Mater. Interfaces*, 2022, **14**, 31951, DOI: 10.1021/acsami.2c06210.

83 S. Parvin, V. Hazra, A. G. Francis, S. K. Pati and S. Bhattacharyya, In situ cation intercalation in the interlayer of tungsten sulfide with overlaying layered double hydroxide in a 2D heterostructure for facile electrochemical redox activity, *Inorg. Chem.*, 2021, **60**, 6911, DOI: 10.1021/acs.inorgchem.1c00011.

84 Y. Yang, W. Zhang, Y. Xiao, Z. Shi, X. Cao, Y. Tang and Q. Gao, $CoNiSe_2$ heteronanorods decorated with layered-double-hydroxides for efficient hydrogen evolution, *Appl. Catal., B*, 2019, **242**, 132, DOI: 10.1016/j.apcatb.2018.09.082.

85 L. Yang, T. Yang, E. Wang, X. Yu, K. Wang, Z. Du, S. Cao, K.-C. Chou and X. Hou, Bifunctional hierarchical NiCoP@FeNi LDH nanosheet array electrocatalyst for industrial-scale high-current-density water splitting, *J. Mater. Sci. Technol.*, 2023, **159**, 33–40, DOI: 10.1016/j.jmst.2023.02.050.

86 M. B. Poudel, N. Logeshwaran, A. R. Kim, S. C. Karthikeyan, S. Vijayapradeep and D. J. Yoo, Integrated core-shell assembly of $Ni_3S_2$ nanowires and CoMoP nanosheets as highly efficient bifunctional electrocatalysts for overall water splitting, *J. Alloys Compd.*, 2023, **960**, 170678, DOI: 10.1016/j.jallcom.2023.170678.

87 H.-Y. Wang, L. Wang, J.-T. Ren, W.-W. Tian, M.-L. Sun and Z.-Y. Yuan, Heteroatom-induced accelerated kinetics on nickel selenide for highly efficient hydrazine-assisted water splitting and Zn-hydrazine battery, *Nanomicro Lett.*, 2023, **15**, 155, DOI: 10.1007/s40820-023-01128-z.

88 S. Khatun and P. Roy, Cobalt chromium vanadium layered triple hydroxides as an efficient oxygen electrocatalyst for alkaline seawater splitting, *Chem. Commun.*, 2022, **58**, 1104, DOI: 10.1039/d1cc05745f.

89 G. Chen, T. Wang, J. Zhang, P. Liu, H. Sun, X. Zhuang, M. Chen and X. Feng, Accelerated hydrogen evolution kinetics on NiFe-layered double hydroxide electrocatalysts by tailoring water dissociation active sites, *Adv. Mater.*, 2018, **30**, 1706279, DOI: 10.1002/adma.201706279.

90 Q. Zhou, Z. Wang, H. Yuan, J. Wang and H. Hu, Rapid hydrogen adsorption-desorption at sulfur sites via an interstitial carbon strategy for efficient HER on $MoS_2$,

*Appl. Catal., B*, 2023, **332**, 122750, DOI: 10.1016/j.apcatb.2023.122750.

91 J. Li, Y. Lv, X. Wu, K. Zhao, H. Zhang, J. Guo and D. Jia, Effectively enhanced activity of hydrogen evolution through strong interfacial coupling on $SnS_2/MoS_2/Ni_3S_2$ heterostructured porous nanosheets, *Colloids Surf., A*, 2023, **670**, 131634, DOI: 10.1016/j.colsurfa.2023.131634.

92 J. Zhang, T. Wang, D. Pohl, B. Rellinghaus, R. Dong, S. Liu, X. Zhuang and X. Feng, Interface Engineering of $MoS_2/Ni_3S_2$ heterostructures for highly enhanced electrochemical overall-water-splitting activity, *Angew. Chem., Int. Ed.*, 2016, **55**, 6702, DOI: 10.1002/anie.201602237.

93 H. Li, S. Chen, Y. Zhang, Q. Zhang, Q. Zhang, X. Jia, L. Gu, X. Sun, L. Song and X. Wang, Systematic design of superaerophobic nanotube-array electrode comprised of transition-metal sulfides for overall water splitting, *Nat. Commun.*, 2018, **9**, 2452, DOI: 10.1038/s41467-018-04888-0.

94 W. Ma, W. Li, H. Zhang and Y. Wang, N-doped carbon wrapped CoFe alloy nanoparticles with $MoS_2$ nanosheets as electrocatalyst for hydrogen and oxygen evolution reactions, *Int. J. Hydrogen Energy*, 2023, **48**, 22032, DOI: 10.1016/j.ijhydene.2023.03.095.

95 Q. Liu, X. Zhao and X. Chen, Single transition metal-decorated C4N/$MoS_2$ heterostructure for boosting oxygen reduction, oxygen evolution, and hydrogen evolution, *J. Colloid Interface Sci.*, 2023, **648**, 787, DOI: 10.1016/j.jcis.2023.06.039.

96 Q. Xie, D. Zhou, P. Li, Z. Cai, T. Xie, T. Gao, R. Chen, Y. Kuang and X. Sun, Enhancing oxygen evolution reaction by cationic surfactants, *Nano Res.*, 2019, **12**, 2302, DOI: 10.1007/s12274-019-2410-z.

97 Z. Wang, W. A. Goddard and H. Xiao, Potential-dependent transition of reaction mechanisms for oxygen evolution on layered double hydroxides, *Nat. Commun.*, 2023, **14**, 4228, DOI: 10.1038/s41467-023-40011-8.

98 F. Dionigi, Z. Zeng, I. Sinev, T. Merzdorf, S. Deshpande, M. B. Lopez, S. Kunze, I. Zegkinoglou, H. Sarodnik, D. Fan, B. Roldan Cuenya and P. Strasser, In-situ structure and catalytic mechanism of NiFe and CoFe layered double hydroxides during oxygen evolution, *Nat. Commun.*, 2020, **11**, 2522, DOI: 10.1038/s41467-020-16237-1.

99 M. Gong and H. Dai, A mini review of NiFe-based materials as highly active oxygen evolution reaction electrocatalysts, *Nano Res.*, 2015, **8**, 23, DOI: 10.1007/s12274-014-0591-z.

100 S. Shin, Z. Jin, D. H. Kwon, R. Bose and Y.-S. Min, High turnover frequency of hydrogen evolution reaction on amorphous $MoS_2$ thin film directly grown by atomic layer deposition, *Langmuir*, 2015, **31**, 1196, DOI: 10.1021/la504162u.

101 Q. Tang and D.-E. Jiang, Mechanism of hydrogen evolution reaction on 1T-$MoS_2$ from first principles, *ACS Catal.*, 2016, **6**, 4953, DOI: 10.1021/acscatal.6b01211.

102 E. E. Benson, H. Zhang, S. A. Schuman, S. U. Nanayakkara, N. D. Bronstein, S. Ferrere, J. L. Blackburn and E. M. Miller, Balancing the hydrogen evolution reaction, surface energetics, and stability of metallic $MoS_2$ nanosheets via covalent functionalization, *J. Am. Chem. Soc.*, 2018, **140**, 441, DOI: 10.1021/jacs.7b11242.

103 S. Deng, M. Luo, C. Ai, Y. Zhang, B. Liu, L. Huang, Z. Jiang, Q. Zhang, L. Gu, S. Lin, X. Xia and J. Tu, Synergistic doping and intercalation: realizing deep phase modulation on $MoS_2$ arrays for high-efficiency hydrogen evolution reaction, *Angew. Chem., Int. Ed.*, 2019, **58**, 16289, DOI: 10.1002/anie.201909698.

104 L. Li, Z. Qin, L. Ries, S. Hong, T. Michel, J. Yang, C. Salameh, M. Bechelany, P. Miele, D. Kaplan, M. Chhowalla and D. Voiry, Role of sulfur vacancies and undercoordinated Mo regions in $MoS_2$ nanosheets toward the evolution of hydrogen, *ACS Nano*, 2019, **13**, 6824, DOI: 10.1021/acsnano.9b01583.

105 Y. Chen, S. Huang, X. Ji, K. Adepalli, K. Yin, X. Ling, X. Wang, J. Xue, M. Dresselhaus, J. Kong, J. Kong and B. Yildiz, Tuning electronic structure of single layer $MoS_2$ through defect and interface engineering, *ACS Nano*, 2018, **12**, 2569, DOI: 10.1021/acsnano.7b08418.

106 R. Li, L. Yang, T. Xiong, Y. Wu, L. Cao, D. Yuan and W. Zhou, Nitrogen doped $MoS_2$ nanosheets synthesized via a low-temperature process as electrocatalysts with enhanced activity for hydrogen evolution reaction, *J. Power Sources*, 2017, **356**, 133, DOI: 10.1016/j.jpowsour.2017.04.060.

107 R. Zhang, M. Zhang, H. Yang, G. Li, S. Xing, M. Li, Y. Xu, Q. Zhang, S. Hu, H. Liao, H. Liao and Y. Cao, Creating fluorine-doped $MoS_2$ edge electrodes with enhanced hydrogen evolution activity, *Small Methods*, 2021, **5**, 2100612, DOI: 10.1002/smtd.202100612.

108 G. Gao, Q. Sun and A. Du, Activating catalytic inert basal plane of molybdenum disulfide to optimize hydrogen evolution activity via defect doping and strain engineering, *J. Phys. Chem. C*, 2016, **120**, 16761, DOI: 10.1021/acs.jpcc.6b04692.

109 R. Bose, M. Seo, C.-Y. Jung and S. C. Yi, Comparative investigation of the molybdenum sulphide doped with cobalt and selenium towards hydrogen evolution reaction, *Electrochim. Acta*, 2018, **271**, 211, DOI: 10.1016/j.electacta.2018.03.151.

110 J. J. L. Humphrey, R. Kronberg, R. Cai, K. Laasonen, R. E. Palmer and A. J. Wain, Active site manipulation in $MoS_2$ cluster electrocatalysts by transition metal doping, *Nanoscale*, 2020, **12**, 4459, DOI: 10.1039/c9nr10702a.

111 H. Shu, D. Zhou, F. Li, D. Cao and X. Chen, Defect engineering in $MoSe_2$ for the hydrogen evolution reaction: from point defects to edges, *ACS Appl. Mater. Interfaces*, 2017, **9**, 42688, DOI: 10.1021/acsami.7b12478.

112 R. Zhao, S. Xu, D. Liu, L. Wei, S. Yang, X. Yan, Y. Chen, Z. Zhou, J. Su, L. Guo, L. Guo and C. Burda, Modulating the electronic structure of NiFe hydroxide by Zr doping enables industrial-grade current densities for water oxidation, *Appl. Catal., B*, 2023, **338**, 123027, DOI: 10.1016/j.apcatb.2023.123027.

113 S. Sun, Y. He, T. Chen, C. Sun and C. Wu, Morphology regulated synthesis of NiFe-layered double hydroxide

 

nanostructures on nickel foam toward efficient oxygen evolution reaction, *J. Alloys Compd.*, 2023, **963**, 171304, DOI: 10.1016/j.jallcom.2023.171304.

114 L. Zhang, X. Yuan, Y. Jin, Y. Liu, L. Tan, H. Chen, K. Huang, Y. Shi and X. Xiong, Simple construction of NiCo–LDH@FeOOH nanoflower heterostructure by chemical etching strategy for efficient oxygen evolution reaction, *J. Alloys Compd.*, 2023, **960**, 170941, DOI: 10.1016/j.jallcom.2023.170941.

115 M. Rong, Y. Mo, S. Zhou, X. Ma, S. Wang, Z. Cao and H. Zhong, Ce and $MoS_2$ dual-doped cobalt aluminum layered double hydroxides for enhanced oxygen evolution reaction, *Int. J. Hydrogen Energy*, 2022, **47**, 1644, DOI: 10.1016/j.ijhydene.2021.10.222.

116 B. Mohanty, M. Ghorbani-Asl, S. Kretschmer, A. Ghosh, P. Guha, S. K. Panda, B. Jena, A. V. Krasheninnikov and B. K. Jena, $MoS_2$ quantum dots as efficient catalyst materials for the oxygen evolution reaction, *ACS Catal.*, 2018, **8**, 1683, DOI: 10.1021/acscatal.7b03180.

117 J.-Y. Xue, F.-L. Li, Z.-Y. Zhao, C. Li, C.-Y. Ni, H.-W. Gu, D. J. Young and J.-P. Lang, In Situ generation of bifunctional Fe-doped $MoS_2$ nanocanopies for efficient electrocatalytic water splitting, *Inorg. Chem.*, 2019, **58**, 11202, DOI: 10.1021/acs.inorgchem.9b01814.

118 Z. Chen, W. Wang, S. Huang, P. Ning, Y. Wu, C. Gao, T.-T. Le, J. Zai, Y. Jiang, Z. Hu, Z. Hu and X. Qian, Well-defined $CoSe_2$@$MoSe_2$ hollow heterostructured nanocubes with enhanced dissociation kinetics for overall water splitting, *Nanoscale*, 2020, **12**, 326, DOI: 10.1039/c9nr08751f.

119 Q. Zhou, Z. Wang, H. Yuan, J. Wang and H. Hu, Rapid hydrogen adsorption-desorption at sulfur sites via an interstitial carbon strategy for efficient HER on $MoS_2$, *Appl. Catal., B*, 2023, **332**, 122750, DOI: 10.1016/j.apcatb.2023.122750.

120 J. Li, K. Li, Q. Tang, J. Liang, C. Bao, F. Shi, M. Fan and J. Jia, Structure phase engineering strategy through acetic acid coupling to boost hydrogen evolution reaction performance of 2H phase $MoS_2$ at wide pH range, *Fuel*, 2023, **347**, 128428, DOI: 10.1016/j.fuel.2023.128428.

121 J. Jiang, X. Wang, X. Liang, J. Zhang and L. Ai, Superwetting molybdenum-based sulfide/phosphide heterostructures for efficient water electrolysis and solar thermoelectricity self-powered hydrogen production, *Appl. Surf. Sci.*, 2023, **631**, 157482, DOI: 10.1016/j.apsusc.2023.157482.

122 W.-B. Jung, G.-T. Yun, Y. Kim, M. Kim and H.-T. Jung, Relationship between hydrogen evolution and wettability for multiscale hierarchical wrinkles, *ACS Appl. Mater. Interfaces*, 2019, **11**, 7546, DOI: 10.1021/acsami.8b19828.

123 J. Gautam, D. Chanda, M. Mekete Meshesha, S. G. Jang and B. Lyong Yang, Manganese cobalt sulfide/molybdenum disulfide nanowire heterojunction as an excellent bifunctional catalyst for electrochemical water splitting, *J. Colloid Interface Sci.*, 2023, **638**, 658, DOI: 10.1016/j.jcis.2023.02.029.

124 N. Pang, Y. Li, X. Tong, M. Wang, H. Shi, D. Wu, D. Xiong, S. Xu, L. Wang, L. Jiang, L. Jiang and P. K. Chu, Activation of basal-plane sulfur sites on $MoS_2$ @$Ni_3S_2$ nanorods by Zr plasma ion implantation for bifunctional electrocatalysts, *J. Alloys Compd.*, 2023, **947**, 157482, DOI: 10.1016/j.jallcom.2023.169448.

125 L. Hui, Y. Xue, B. Huang, H. Yu, C. Zhang, D. Zhang, D. Jia, Y. Zhao, Y. Li, H. Liu, H. Liu and Y. Li, Overall water splitting by graphdiyne-exfoliated and -sandwiched layered double-hydroxide nanosheet arrays, *Nat. Commun.*, 2018, **9**, 5309, DOI: 10.1038/s41467-018-07790-x.

126 H. Yu, C. Chen, N. Yu, K. Feng, X. Zhang, N. Cai, Y. Xue, H. Li, J. Wang and F. Yu, Graphene-templated growth of $MoS_2$/$Ni_3S_2$ heterostructures as efficient electrocatalysts for overall water splitting, *Colloids Surf., A*, 2023, **658**, 130550, DOI: 10.1016/j.colsurfa.2022.130550.

127 I. Ahmed, R. Biswas, M. Iqbal, A. Roy and K. K. Haldar, NiS/$MoS_2$ Anchored multiwall carbon nanotube electrocatalyst for hydrogen generation and energy storage applications, *ChemNanoMat*, 2023, **9**, e202200550, DOI: 10.1002/cnma.202200550.

128 T. L. L. Doan, D. C. Nguyen, S. Prabhakaran, D. H. Kim, D. T. Tran, N. H. Kim and J. H. Lee, Single-atom co-decorated $MoS_2$ nanosheets assembled on metal nitride nanorod arrays as an efficient bifunctional electrocatalyst for pH-universal water splitting, *Adv. Funct. Mater.*, 2021, **31**, 2100233, DOI: 10.1002/adfm.202100233.

129 J. Ma, A. Cai, X. Guan, K. Li, W. Peng, X. Fan, G. Zhang, F. Zhang and Y. Li, Preparation of ultrathin molybdenum disulfide dispersed on graphene via cobalt doping: A bifunctional catalyst for hydrogen and oxygen evolution reaction, *Int. J. Hydrogen Energy*, 2020, **45**, 9583, DOI: 10.1016/j.ijhydene.2020.01.176.

130 Q. Wei, D. Wang, L. Zhang, L. Zhao, B. Zhang, G. Zhou and Y. Zhao, Fabrication of Co doped $MoS_2$ nanosheets with enlarged interlayer spacing as efficient and pH-Universal bifunctional electrocatalyst for overall water splitting, *Ceram. Int.*, 2021, **47**, 24501, DOI: 10.1016/j.ceramint.2021.05.166.

131 Y. Yang, H. Yao, Z. Yu, S. M. Islam, H. He, M. Yuan, Y. Yue, K. Xu, W. Hao, G. Sun, P. Zapol and M. G. Kanatzidis, Hierarchical Nanoassembly of $MoS_2$/$Co_9S_8$/$Ni_3S_2$/Ni as a highly efficient electrocatalyst for overall water splitting in a wide pH range, *J. Am. Chem. Soc.*, 2019, **141**, 10417, DOI: 10.1021/jacs.9b04492.

132 R. K. Mishra, V. Kumar, L. G. Trung, G. J. Choi, J. W. Ryu, P. Kumar, R. Bhardwaj, S. H. Lee and J. S. Gwag, Bifunctionality of $MoS_2$ nanolayer catalyst for water-splitting reactions of hydrogen and oxygen, *Mater. Lett.*, 2023, **338**, 134026, DOI: 10.1016/j.matlet.2023.134026.

133 S. Wang, X. Ning, Y. Cao, R. Chen, Z. Lu, J. Hu, J. Xie and A. Hao, Construction of an Advanced NiFe–LDH/$MoS_2$–$Ni_3S_2$/NF heterostructure catalyst toward efficient electrocatalytic overall water splitting, *Inorg. Chem.*, 2023, **62**, 6428, DOI: 10.1021/acs.inorgchem.3c00425.

134 M. Wu, X. Meng, M. Zhou and Y. Zhou, Cobalt incorporation and $MoS_2$–$NiS_2$ heterostructure synergistic for improving full water electrolysis efficiency, *New J. Chem.*, 2023, **47**, 9492, DOI: 10.1039/d3nj00755c.

135 J. Lin, P. Wang, H. Wang, C. Li, X. Si, J. Qi, J. Cao, Z. Zhong, W. Fei and J. Feng, Defect-rich heterogeneous $MoS_2NiS_2$ nanosheets electrocatalysts for efficient overall water splitting, *Adv. Sci.*, 2019, **6**, 1900246, DOI: **10.1002/advs.201900246**.

136 Q. Xiong, Y. Wang, P.-F. Liu, L.-R. Zheng, G. Wang, H.-G. Yang, P.-K. Wong, H. Zhang and H. Zhao, Cobalt covalent doping in $MoS_2$ to induce bifunctionality of overall water splitting, *Adv. Mater.*, 2018, **30**, 1801450, DOI: **10.1002/adma.201801450**.

137 A. Muthurasu, V. Maruthapandian and H. Y. Kim, Metal-organic framework derived Co3O4/$MoS_2$ heterostructure for efficient bifunctional electrocatalysts for oxygen evolution reaction and hydrogen evolution reaction, *Appl. Catal., B*, 2019, **248**, 202, DOI: **10.1016/j.apcatb.2019.02.014**.

138 P. Kuang, M. He, H. Zou, J. Yu and K. Fan, 0D/3D $MoS_2$–$NiS_2$/N-doped graphene foam composite for efficient overall water splitting, *Appl. Catal., B*, 2019, **254**, 15, DOI: **10.1016/j.apcatb.2019.04.072**.

139 M. Zheng, K. Guo, W.-J. Jiang, T. Tang, X. Wang, P. Zhou, J. Du, Y. Zhao, C. Xu and J.-S. Hu, When $MoS_2$ meets FeOOH: A ''one-stone-two-birds'' heterostructure as a bifunctional electrocatalyst for efficient alkaline water splitting, *Appl. Catal., B*, 2019, **244**, 1004, DOI: **10.1016/j.apcatb.2018.12.019**.

140 Y. Li, C. Wang, M. Cui, J. Xiong, L. Mi and S. Chen, Heterostructured MoO2@$MoS_2$@$Co_9S_8$ nanorods as high efficiency bifunctional electrocatalyst for overall water splitting, *Appl. Surf. Sci.*, 2021, **543**, 148804, DOI: **10.1016/j.apsusc.2020.148804**.

141 R. Yang, Y. Zhou, Y. Xing, D. Li, D. Jiang, M. Chen, W. Shi and S. Yuan, Synergistic coupling of CoFe–LDH arrays with NiFe–LDH nanosheet for highly efficient overall water splitting in alkaline media, *Appl. Catal., B*, 2019, **253**, 131, DOI: **10.1016/j.apcatb.2019.04.054**.

142 X. Wang, Y. Yang, L. Diao, Y. Tang, F. He, E. Liu, C. He, C. Shi, J. Li, J. Sha, L. Ma and N. Zhao, CeOx-decorated NiFe-layered double hydroxide for efficient alkaline hydrogen evolution by oxygen vacancy engineering, *ACS Appl. Mater. Interfaces*, 2018, **10**, 35145, DOI: **10.1021/acsami.8b11688**.

143 R. Fan, Q. Mu, Z. Wei, Y. Peng and M. Shen, Atomic Ir-doped NiCo layered double hydroxide as a bifunctional electrocatalyst for highly efficient and durable water splitting, *J. Mater. Chem. A*, 2020, **8**, 9871, DOI: **10.1039/d0ta03272g**.

144 J. Bao, Z. Wang, J. Xie, L. Xu, F. Lei, M. Guan, Y. Zhao, Y. Huang and H. Li, A ternary cobalt-molybdenum-vanadium layered double hydroxide nanosheet array as an efficient bifunctional electrocatalyst for overall water splitting, *Chem Comm*, 2019, **55**, 3521, DOI: **10.1039/C9CC00269C**.

145 P. Wang, J. Qi, X. Chen, C. Li, W. Li, T. Wang and C. Liang, Three-dimensional heterostructured NiCoP@NiMn-layered double hydroxide arrays supported on Ni foam as a bifunctional electrocatalyst for overall water splitting, *ACS Appl. Mater. Interfaces*, 2020, **12**, 4385, DOI: **10.1021/acsami.9b15208**.

146 W. Mai, Q. Cui, Z. Zhang, K. Zhang, G. Li, L. Tian and W. Hu, CoMoP/NiFe-layered double-hydroxide hierarchical nanosheet arrays standing on Ni foam for efficient overall water splitting, *ACS Appl. Energy Mater.*, 2020, **3**, 8075, DOI: **10.1021/acsaem.0c01538**.

147 L. Yin, X. Du, C. Di, M. Wang, K. Su and Z. Li, In-situ transformation obtained defect-rich porous hollow CuO@-CoZn–LDH nanoarrays as self-supported electrode for highly efficient overall water splitting, *Chem Eng J.*, 2021, **414**, 128809, DOI: **10.1016/j.cej.2021.128809**.

148 K. Chen, Y.-H. Cao, S. Yadav, G.-C. Kim, Z. Han, W. Wang, W.-J. Zhang, V. Dao and I.-H. Lee, Electronic structure reconfiguration of nickel–cobalt layered double hydroxide nanoflakes via engineered heteroatom and oxygen-vacancies defect for efficient electrochemical water splitting, *Chem Eng J.*, 2023, **463**, 142396, DOI: **10.1016/j.cej.2023.142396**.

149 X. Lyu, Y. Zhang, X. Wang, H. Chen, S. Li, W. Zhang, Y. Hu, F. Li, D. Li and D. Yang, Electronic structure regulation of nickel-iron layered double hydroxides by tuning ternary component for overall water splitting, *Mater. Today Sustainability*, 2023, **21**, 100295, DOI: **10.1016/j.mtsust.2022.100295**.

150 S. Zhang, Y. Wang, S. Li, Z. Wang, H. Chen, L. Yi, X. Chen, Q. Yang, W. Xu, A. Wang, A. Wang and Z. Lu, Concerning the stability of seawater electrolysis: a corrosion mechanism study of halide on Ni-based anode, *Nat. Commun.*, 2023, **14**, 4822, DOI: **10.1038/s41467-023-40563-9**.

151 M. Islam, T. H. Nguyen, D. T. Tran, V. A. Dinh, N. H. Kim and J. H. Lee, Bimetallic atom dual-doped $MoS_2$-based heterostructures as a high-efficiency catalyst to boost solar-assisted alkaline seawater electrolysis, *ACS Sustainable Chem. Eng.*, 2023, **11**, 6688, DOI: **10.1021/acssuschemeng.3c00260**.

152 M. S. Kim, D. T. Tran, T. H. Nguyen, V. A. Dinh, N. H. Kim and J. H. Lee, Ni single atoms and Ni phosphate clusters synergistically triggered surface-functionalized $MoS_2$ nanosheets for high-performance freshwater and seawater electrolysis, *Energy Environ. Mater.*, 2022, **5**, 1340, DOI: **10.1002/eem2.12366**.

153 S. Song, Y. Wang, S. Zhou, H. Gao, X. Tian, Y. Yuan, W. Li and J. Zang, One-step synthesis of heterostructural $MoS_2$-(FeNi)9S8 on Ni-Fe foam synergistically boosting for efficient fresh/seawater electrolysis, *ACS Appl. Energy Mater.*, 2022, **5**, 1810, DOI: **10.1021/acsaem.1c03015**.

154 Y. Gong, H. Zhao, Y. Sun, D. Xu, D. Ye, Y. Tang, T. He and J. Zhang, Partially selenized FeCo layered double hydroxide as bifunctional electrocatalyst for efficient and stable alkaline (sea)water splitting, *J. Colloid Interface Sci.*, 2023, **650**, 636, DOI: **10.1016/j.jcis.2023.07.013**.

155 S. Zhou, J. Wang, J. Li, L. Fan, Z. Liu, J. Shi and W. Cai, Surface-growing organophosphorus layer on layered double hydroxides enables boosted and durable electrochemical freshwater/seawater oxidation, *Appl. Catal., B*, 2023, **332**, 122749, DOI: **10.1016/j.apcatb.2023.122749**.

156 M. Li, H.-J. Niu, Y. Li, J. Liu, X. Yang, Y. Lv, K. Chen and W. Zhou, Synergetic regulation of $CeO_2$ modification and (W2O7)2- intercalation on NiFe–LDH for high-performance large-current seawater electrooxidation, *Appl. Catal., B*, 2023, **330**, 122612, DOI: **10.1016/j.apcatb.2023.122612**.

157 Y. Zhang, P. Gao, W. Yu, Z. Yan, Q. Chen, L. Luo, M. Wang and Y. Chen, Cu2S nanorods decorated with NiFe-layered double hydroxide nanosheets as bifunctional electrocatalysts for hydrogen evolution in alkaline saline water/seawater, *ACS Appl. Nano Mater.*, 2023, **6**, 9816, DOI: **10.1021/acsanm.3c01555**.

158 E. Enkhtuvshin, S. Yeo, H. Choi, K. M. Kim, B.-S. An, S. Biswas, Y. Lee, A. K. Nayak, J. U. Jang, K.-H. Na, C.-Y. Chung and H. Han, Surface reconstruction of Ni–Fe layered double hydroxide inducing chloride ion blocking materials for outstanding overall seawater splitting, *Adv. Funct. Mater.*, 2023, **33**, 2214069, DOI: **10.1002/adfm.202214069**.

159 N. Kitiphatpiboon, M. Chen, C. Feng, Y. Zhou, C. Liu, Z. Feng, Q. Zhao, A. Abudula and G. Guan, Modification of spinel MnCo2O4 nanowire with NiFe-layered double hydroxide nanoflakes for stable seawater oxidation, *J. Colloid Interface Sci.*, 2023, **632**, 54, DOI: **10.1016/j.jcis.2022.11.044**.

160 B. Zhang, S. Liu, S. Zhang, Y. Cao, H. Wang, C. Han and J. Sun, High Corrosion resistance of NiFe-layered double hydroxide catalyst for stable seawater electrolysis promoted by phosphate intercalation, *Small*, 2022, **18**, 2203852, DOI: **10.1002/smll.202203852**.

161 H. Sun, L. Li, H.-C. Chen, D. Duan, M. Humayun, Y. Qiu, X. Zhang, X. Ao, Y. Wu, Y. Pang, C. Wang and Y. Xiong, Highly efficient overall urea electrolysis via single-atomically active centers on layered double hydroxide, *Sci. Bull.*, 2022, **67**, 1763, DOI: **10.1016/j.scib.2022.08.008**.

162 S. Sheng, K. Ye, Y. Gao, K. Zhu, J. Yan, G. Wang and D. Cao, Simultaneously boosting hydrogen production and ethanol upgrading using a highly-efficient hollow needle-like copper cobalt sulfide as a bifunctional electrocatalyst, *J. Colloid Interface Sci.*, 2021, **602**, 325, DOI: **10.1016/j.jcis.2021.06.001**.

163 Z. G. Schichtl, S. K. Conlin, H. Mehrabi, A. C. Nielander and R. H. Coridan, Characterizing sustained solar-to-hydrogen electrocatalysis at low cell potentials enabled by crude glycerol oxidation, *ACS Appl. Energy Mater.*, 2022, **5**, 3863, DOI: **10.1021/acsaem.2c00377**.

164 N. Jiang, X. Liu, J. Dong, B. You, X. Liu and Y. Sun, Electrocatalysis of furfural oxidation coupled with H2 evolution via nickel-based electrocatalysts in water, *ChemNanoMat*, 2017, **3**, 491, DOI: **10.1002/cnma.201700076**.

165 Y. Ding, X. Du and X. Zhang, Rose-like Cu-doped $Ni_3S_2$ nanoflowers decorated with thin NiFe LDH nanosheets for high-efficiency overall water and urea electrolysis, *Appl. Surf. Sci.*, 2022, **584**, 152622, DOI: **10.1016/j.apsusc.2022.152622**.

166 H. Sun, W. Zhang, J.-G. Li, Z. Li, X. Ao, K.-H. Xue, K. K. Ostrikov, J. Tang and C. Wang, Rh-engineered ultrathin NiFe–LDH nanosheets enable highly-efficient overall water splitting and urea electrolysis, *Appl. Catal., B*, 2021, **284**, 152622, DOI: **10.1016/j.apcatb.2020.119740**.

167 D. Khalafallah, L. Xiaoyu, M. Zhi and Z. Hong, 3D hierarchical NiCo layered double hydroxide nanosheet arrays decorated with noble metal nanoparticles for enhanced urea eectrocatalysis, *ChemElectroChem*, 2020, **7**, 163, DOI: **10.1002/celc.201901423**.

168 J. Wei, J. Wang and X. Sun, $H_2O_2$ treatment boosts activity of NiFe layered double hydroxide for electro-catalytic oxidation of urea, *J. Environ. Sci.*, 2023, **129**, 152, DOI: **10.1016/j.jes.2022.08.023**.

169 D. Li, X. Zhou, L. Liu, Q. Ruan, X. Zhang, B. Wang, F. Xiong, C. Huang and P. K. Chu, Reduced anodic energy depletion in electrolysis by urea and water co-oxidization on NiFe–LDH: Activity origin and plasma functionalized strategy, *Appl. Catal., B*, 2023, **324**, 122240, DOI: **10.1016/j.apcatb.2022.122240**.

170 M. Zeng, J. Wu, Z. Li, H. Wu, J. Wang, H. Wang, L. He and X. Yang, Interlayer effect in NiCo layered double hydroxide for promoted electrocatalytic urea oxidation, *ACS Sustainable Chem. Eng.*, 2019, **7**, 4777, DOI: **10.1021/acssuschemeng.8b04953**.

171 Y. X. Chen, A. Lavacchi, H. A. Miller, M. Bevilacqua, J. Filippi, M. Innocenti, A. Marchionni, W. Oberhauser, L. Wang and F. Vizza, Nanotechnology makes biomass electrolysis more energy efficient than water electrolysis, *Nat. Commun.*, 2014, **5**, 4036, DOI: **10.1038/ncomms5036**.

172 N. Shilpa, A. Pandikassala, P. Krishnaraj, P. S. Walko, R. N. Devi and S. Kurungot, Co–Ni layered double hydroxide for the electrocatalytic oxidation of organic molecules: An approach to lowering the overall cell voltage for the water splitting process, *ACS Appl. Mater. Interfaces*, 2022, **14**, 16222, DOI: **10.1021/acsami.2c00982**.

173 Y. Ding, Q. Xue, Q.-L. Hong, F.-M. Li, Y.-C. Jiang, S.-N. Li and Y. Chen, Hydrogen and potassium acetate co-production from electrochemical reforming of ethanol at ultrathin cobalt sulfide nanosheets on nickel foam, *ACS Appl. Mater. Interfaces*, 2021, **13**, 4026, DOI: **10.1021/acsami.0c20554**.